



HAL
open science

Evolutionary Gain of Dbx1 Expression Drives Subplate Identity in the Cerebral Cortex

Yoko Arai, Andrzej Cwetsch, Eva Coppola, Sara Cipriani, Hidenori Nishihara, Hiroaki Kanki, Yoann Saillour, Betty Freret-Hodara, Annie Dutriaux, Norihiro Okada, et al.

► **To cite this version:**

Yoko Arai, Andrzej Cwetsch, Eva Coppola, Sara Cipriani, Hidenori Nishihara, et al.. Evolutionary Gain of Dbx1 Expression Drives Subplate Identity in the Cerebral Cortex. *Cell Reports*, 2019, 29 (3), pp.645-658.e5. 10.1016/j.celrep.2019.09.007 . hal-02322661

HAL Id: hal-02322661

<https://hal.science/hal-02322661>

Submitted on 14 Dec 2020

HAL is a multi-disciplinary open access archive for the deposit and dissemination of scientific research documents, whether they are published or not. The documents may come from teaching and research institutions in France or abroad, or from public or private research centers.

L'archive ouverte pluridisciplinaire **HAL**, est destinée au dépôt et à la diffusion de documents scientifiques de niveau recherche, publiés ou non, émanant des établissements d'enseignement et de recherche français ou étrangers, des laboratoires publics ou privés.

Evolutionary Gain of *Dbx1* Expression Drives Subplate Identity in the Cerebral Cortex

Yoko Arai,^{3,12,13} Andrzej W. Cwetsch,^{1,2} Eva Coppola,^{1,2,3} Sara Cipriani,⁴ Hidenori Nishihara,⁵ Hiroaki Kanki,⁶ Yoann Saillour,^{1,2} Betty Freret-Hodara,³ Annie Dutriaux,³ Norihiro Okada,⁷ Hideyuki Okano,^{6,8} Colette Dehay,⁹ Jeannette Nardelli,⁴ Pierre Gressens,⁴ Tomomi Shimogori,¹⁰ Giuseppe D'Onofrio,¹¹ and Alessandra Pierani^{1,2,3,14,*}

¹Imagine Institute of Genetic Diseases, Université de Paris, Paris 75015, France

²Institute of Psychiatry and Neuroscience of Paris, INSERM U1266, Université de Paris, Paris 75014, France

³Institut Jacques Monod, CNRS UMR 7592, Université de Paris, 75205 Paris Cedex, France

⁴Université de Paris, NeuroDiderot, INSERM, Paris 75019, France

⁵Department of Life Science and Technology, Tokyo Institute of Technology, Yokohama 226-8501, Japan

⁶Department of Physiology, Keio University School of Medicine, Tokyo 160-8582, Japan

⁷Foundation for Advancement of International Science, Tsukuba 305-0821, Japan

⁸Laboratory for Marmoset Neural Architecture, RIKEN Center for Brain Science, Wako, Saitama 351-0198, Japan

⁹Université Lyon, Université Claude Bernard Lyon 1, INSERM, Stem Cell and Brain Research Institute U1208, 69500 Bron, France

¹⁰Molecular Mechanisms of Brain Development, RIKEN Center for Brain Science, Wako, Saitama 351-0198, Japan

¹¹Department BEOM, Stazione Zoologica A. Dohrn, Napoli 80121, Italy

¹²Present address: Center for Interdisciplinary Research in Biology, Collège de France, CNRS UMR Paris-Sciences-Lettres 7241, INSERM U1050, Labex Memolife, PSL Research University, Paris 75005, France

¹³Present address: BrainEver, Paris 75005, France

¹⁴Lead Contact

*Correspondence: alessandra.pierani@inserm.fr

<https://doi.org/10.1016/j.celrep.2019.09.007>

SUMMARY

Changes in transcriptional regulation through *cis*-regulatory elements are thought to drive brain evolution. However, how this impacts the identity of primate cortical neurons is still unresolved. Here, we show that primate-specific *cis*-regulatory sequences upstream of the *Dbx1* gene promote human-like expression in the mouse embryonic cerebral cortex, and this imparts cell identity. Indeed, while *Dbx1* is expressed in highly restricted cortical progenitors in the mouse ventral pallium, it is maintained in neurons in primates. Phenocopy of the primate-like *Dbx1* expression in mouse cortical progenitors induces ectopic Cajal-Retzius and subplate (SP) neurons, which are transient populations playing crucial roles in cortical development. A conditional expression solely in neurons uncouples mitotic and postmitotic activities of *Dbx1* and exclusively promotes a SP-like fate. Our results highlight how transcriptional changes of a single fate determinant in postmitotic cells may contribute to the expansion of neuronal diversity during cortical evolution.

INTRODUCTION

The human cerebral cortex differs substantially with regards to anatomy and function compared to other mammalian species. During evolution, enhanced cognitive abilities are associated with a complexification of neuronal networks in the cerebral cortex (Arai and Pierani, 2014; Hill and Walsh, 2005; Rakic, 2009).

Early-born Cajal-Retzius (CR) and subplate (SP) neurons pioneer the formation of these neuronal circuits during development (Rakic, 2009; Arai and Pierani, 2014; Meyer, 2010; Hoerder-Sua-bedissen and Molnár, 2015), and a pronounced gain in both their number and subtype diversity has been linked with cortical evolution (Arai and Pierani, 2014; Meyer, 2010; Hoerder-Sua-bedissen and Molnár, 2015; Zecevic and Rakic, 2001; Smart et al., 2002). While the increase in the number of neurons is correlated with the expansion of progenitor pools (Hansen et al., 2010; Fietz et al., 2010; Betizeau et al., 2013), how the diversity of cortical neuron subtypes arises is still an open question.

In the mouse, CR neurons are among the first-generated glutamatergic neurons between embryonic day 10.5 (E10.5) and E12.5. They are derived from progenitors located at the borders of the developing cerebral cortex (or pallium): (1) the ventral pallium (VP) dorsal to the pallial-subpallial boundary (PSB), (2) the pallial septum (hereafter septum), and (3) the cortical hem (Bielle et al., 2005; Takiguchi-Hayashi et al., 2004; Yoshida et al., 2006; Barber and Pierani, 2016). CR neurons migrate tangentially to cover the entire cortical surface and form the preplate, together with SP neurons (Supèr et al., 1998; Meyer et al., 1999). SP neurons are also born within a very restricted developmental window between E11.5 and E13 (Price et al., 1997), from progenitors located in the dorsal pallium (DP) and rostromedial telencephalic wall (Pedraza et al., 2014), and migrate radially and tangentially into the preplate, respectively. The preplate is subsequently split into the marginal zone (MZ) and the SP by the incoming radially migrating cortical pyramidal neurons, which will form the cortical plate (Kwan et al., 2012). CR neurons thus populate the superficial MZ (future layer 1), while SP neurons reside below the cortical plate (Supèr et al., 1998). CR neurons secrete Reelin (Reln), an extracellular matrix glycoprotein, and deletion of the *reelin* gene in the mouse results in a disorganization of the cortical laminar



formation (D'Arcangelo et al., 1995; Ogawa et al., 1995). Molecularly and functionally distinct CR subtypes have been identified (Bielle et al., 2005; Takiguchi-Hayashi et al., 2004; Tissir et al., 2009; Yoshida et al., 2006), and the role of their specific distribution in patterning of cortical areas has emerged, including in controlling the size and connectivity of higher-order areas in the cerebral cortex, whose expansion is a hallmark of cortical evolution (Griveau et al., 2010; Barber et al., 2015). SP neurons are necessary for thalamocortical axons pathfinding and intracortical circuit formation (Ghosh et al., 1990; Hoerder-Suabedissen and Molnár, 2015; McConnell et al., 1989). The absence of SP neurons in the *Gli3* mouse mutant (*Gli3^{Xt/Pdn}*) also results in the defective development of corticofugal axons (Magnani et al., 2013). The function of CR and SP neurons is therefore crucial for the correct cortical organization and circuit formation beginning from the earliest stages of corticogenesis.

The transcription factor developing brain homeobox 1, *Dbx1*, is expressed in two CR generation sites at the VP/PSB and septum (S) (Bielle et al., 2005). The genetic ablation of *Dbx1*-derived CR neurons resulted in a positional shift of postnatal primary cortical areas (Griveau et al., 2010), highlighting the importance of *Dbx1*-derived CR neurons in cortical arealization. In addition to the role of *Dbx1*-derived CR neurons, a modification of *Dbx1* expression in the cerebral cortex was identified by comparison between chick and mouse embryos suggesting that *Dbx1* expression at the VP/PSB is acquired in mice (Bielle et al., 2005) and may underlie the increased generation of CR neurons along the mammalian lineage (Bar et al., 2000; Nomura et al., 2008). While *Dbx1* was shown to function as a potent cell-fate determinant in the mouse spinal cord (Pierani et al., 2001), rhombencephalon (Bouvier et al., 2010), and diencephalon (Sokolowski et al., 2015), the role of *Dbx1* in the cerebral cortex and further during cortical evolution is largely unknown.

In the present study, we identified a substantial difference in the expression pattern of the *Dbx1* gene between primates (human and macaque) and mouse both in progenitors and neurons at the VP/PSB. We correlated this novel expression pattern with the acquisition of primate-specific *cis*-regulatory elements. In order to understand the evolutionary relevance of the *Dbx1* expression gain, we mimicked a primate-like expression of *Dbx1* in the mouse cerebral cortex. While *Dbx1* overexpression in progenitors induced both CR and SP fate, specific postmitotic expression determined a switch to a SP-like identity, which is not observed in *Dbx1*-derived neurons in the mouse. Our data point to a key control of preplate neurons identity occurring in postmitotic cells. They suggest that during cortical evolution the modification of the expression site of a single cell-fate determinant through primate-specific sequences may have a significant impact on the number and diversity of the earliest-born neurons, which are crucial organizers of cortical wiring.

RESULTS

Gain of *Dbx1* Expression Sites in the Primate Developing Cortex

To investigate the evolutionary role of *Dbx1*, we examined *Dbx1* expression in the developing human cortex at Carnegie

stage 18–19 (CS18–CS19)/gestational week (GW) 6.5. We detected *Dbx1* expression at two CR generation sites: the VP located just dorsal to the PSB, defined by the limit of Pax6 expression (Figures 1A–1I) (Puelles and Rubenstein, 1993), and the pallial septum, defined by *Tbr1* expression (Figures S1A–S1D; refer to Bayer and Altman, 2002). In the human septum, *Dbx1* was expressed in progenitors and in young *Reln* (*Reln*⁺) CR neurons (Figure S1B) as observed in the mouse (Griveau et al., 2010), suggesting a conserved *Dbx1* expression in the septum throughout evolution. At the VP, however, *Dbx1* expression extended dorsally into pallial territories (hereafter called DP for simplicity) as determined by the expression of the Pax6 and *Tbr1* proteins (Figures 1B–1E). Moreover, *Dbx1* was found in the proliferative subventricular zone (SVZ) (Figures 1F and 1I) and at high levels in the postmitotic compartment (Figures 1G–1I, S1E, and S1F), as defined by Pax6, *Tbr2*, and *Ctip2/Tbr1* expression in the VZ, SVZ, and postmitotic compartment (NL) (Betizeau et al., 2013; Englund et al., 2005), respectively. Our analysis in human embryos corresponded to a stage when preplate neurons, including CR neurons (Meyer et al., 2000), were already generated. Furthermore, we found that *Dbx1* was expressed in both *Reln*⁺ CR neurons and *Reln*[−] neurons, the latter overlapping with markers of early-born neurons *Ctip2* and *Tbr1* (Figures 1G–1I). This contrasted with the transient *Dbx1* expression confined to progenitors in the mouse VP/PSB (Figure S1G) (Bielle et al., 2005; Griveau et al., 2010; Teissier et al., 2010). Transcriptome profiling in human fetuses (BrainSpan, 2011) at later stages of development showed postmitotic expression of *Dbx1* in the cingulate MZ/cortical plate (<http://brainspan.org/lcm/gene/78785>), in agreement with our observations. We could not detect any *Dbx1* expression in two additional human fetuses at GW5.5 and GW6.0 as well as in human datasets available (for *in situ* hybridization data, the Allen developing human and developing non-human primate brain atlases, the Marmoset gene atlas, and HuDSeN) or in a dozen single-cell RNA sequencing (scRNA-seq) datasets (human and non-human primates, tissues, and organoids), either accessible through web browser (UCSC cell browser or ShinyCortex) or downloaded from the GEO repository. Collectively, these results suggest a low and very restricted *Dbx1* expression in humans both spatially and temporally.

To further characterize *Dbx1* expression in primates, we analyzed a similar area close to the PSB (*Tbr2*⁺ region) in the macaque at E49 and observed *Dbx1*⁺ neurons co-expressing *Reln* and/or *Calr* in the postmitotic compartment (Figures 1J–1L). *Dbx1*⁺*Reln*⁺ and *Dbx1*⁺*Calr*⁺ neurons were also observed in a second macaque fetus at E48 (Figures S1H–S1K) in pallial territories as determined by *Tbr2* expression. We were unable to observe an expression in the SVZ as in the human fetus. This may be due either to the fact that *Dbx1* is expressed in the SVZ at the VP/PSB in a very restricted area only detected in few sagittal sections or to differences between macaque and human. These results suggest that *Dbx1* expression at the VP is under specific regulation, being acquired at some stage of mammalian evolution first in progenitors and then maintained in differentiated neurons.

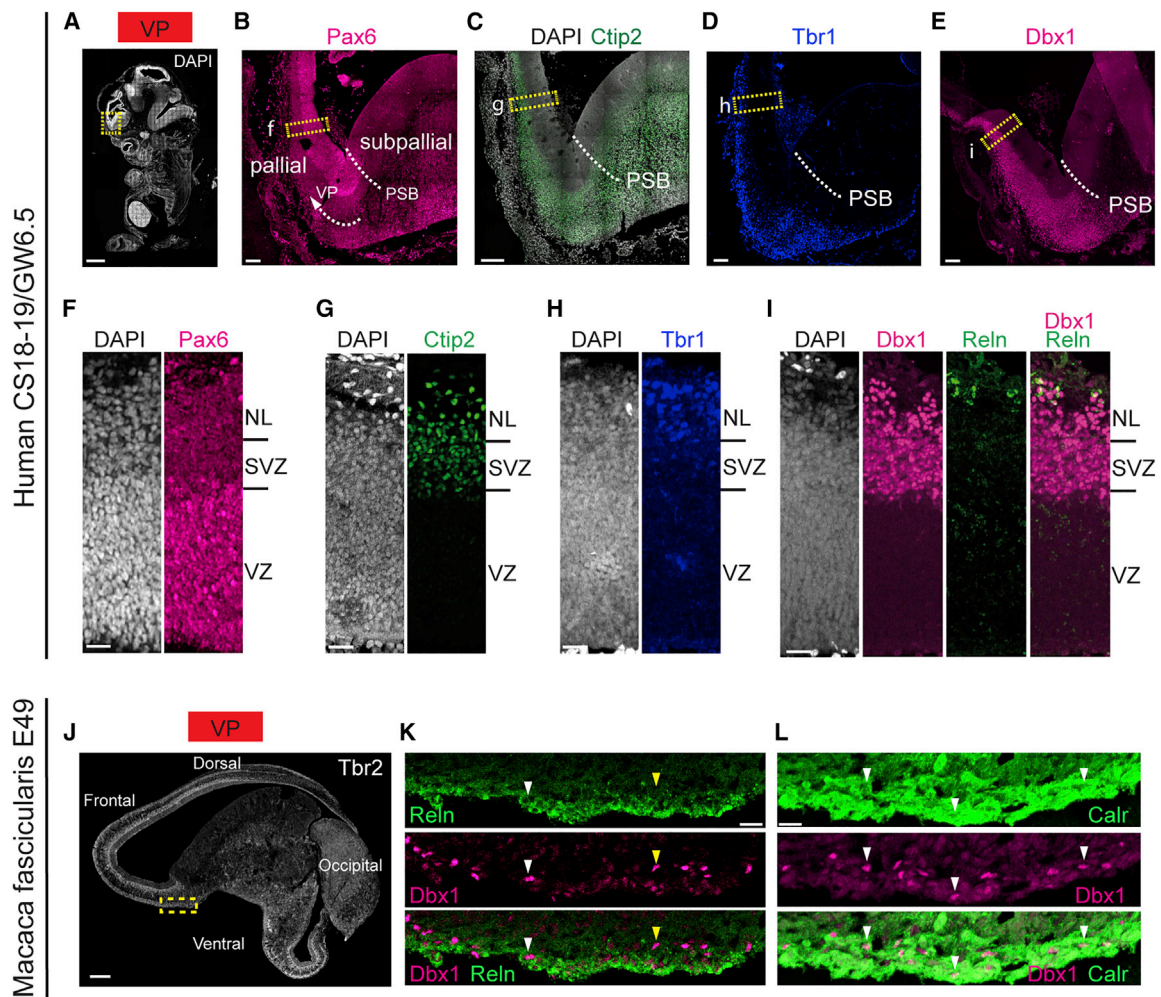


Figure 1. *Dbx1* Expression in the Developing Human and Macaque Fetuses

(A–I) Sagittal cryosections of a CS18/GW6.5 human embryo.

(A) DAPI staining at lateral level. A yellow-dashed box shows the VP.

(B–E) Pax6 (B), Ctip2 (C), Tbr1 (D), and Dbx1 (E) immunofluorescence combined with DAPI (C) at the VP using sections adjacent to (B). Pax6 is expressed in the pallium dorsal to the PSB. White-dashed lines show the PSB.

(F–I) High magnifications of yellow-dashed boxes shown in (B)–(E). Pax6 (F), Ctip2 (G), Tbr1 (H), and Dbx1 and Reln (I) immunofluorescence combined with DAPI staining. Dbx1 co-labels with Reln in the postmitotic compartment (preplate/marginal zone) and is expressed in the SVZ, which is defined by Pax6, Ctip2, and Tbr1 expression (Pax6^{low}Ctip2⁺Tbr1⁻).

(J–L) Sagittal cryosection of an E49 macaque embryo.

(J) Tbr2 immunofluorescence; Tbr2 expression shows pallial territories.

(K) Dbx1 and Reln immunofluorescence. High magnification of the yellow-dashed box at the ventral pallium in (J) shows the neuronal layer close to the pallial-subpallial boundary. Examples of Dbx1 and Reln⁺ immunopositive CRs (white arrowheads) and Dbx1⁺Reln⁻ cortical neurons (yellow arrowheads).

(L) Dbx1 and Calr immunofluorescence of an equivalent area in a section adjacent to (K). Dbx1⁺Calr⁺ CRs (white arrowheads).

VZ, ventricular zone; SVZ, subventricular zone; NL, neuronal layer; VP, ventral pallium; PSB, pallial-subpallial boundary.

Scale bars represent 2 mm (A), 100 μ m (B–E), 25 μ m (F–I), 500 μ m (J), and 10 μ m (K and L).

Primate-Specific Upstream Sequences to the *Dbx1* Gene Drive Ectopic EGFP Expression in the Mouse DP

To gain insight into the potential mechanism of the primate-specific regulation of *Dbx1* expression, we performed a comparative analysis of mammalian genomic regions upstream of the gene. The genomic sequence upstream of the *Dbx1* gene spanning –10 to –5 kb upstream of the *Dbx1* transcription start site contained a unique signature well conserved in primates when

compared to non-primate species, such as carnivores (ferret) and rodents (mouse) (Figure 2A). The proximal –5 kb upstream elements were highly conserved across all mammals and were previously shown by transgenic analyses to recapitulate the endogenous murine *Dbx1* expression (Figure 2A) (Lu et al., 1996).

To study the transcriptional activity of the primate-specific genomic elements, we compared the expression of three

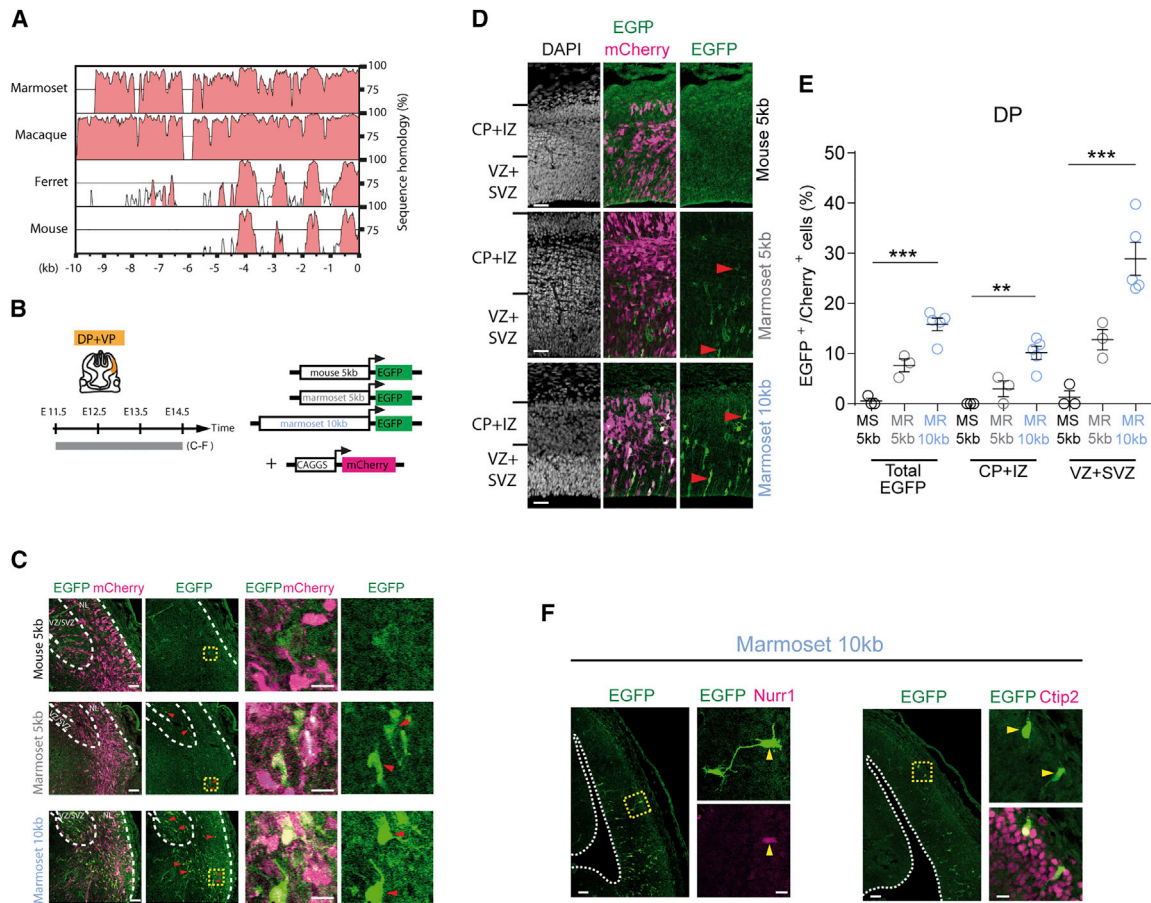


Figure 2. The 10 kb Primate Upstream Sequences Drive Transcription in Both Progenitors and Neurons

(A) Plot showing the pairwise alignment of the human *Dbx1* 10 kb 5'-flanking regions against the corresponding sequences of marmoset, macaque, ferret, and mouse.

(B) Experimental design. Wild-type mouse embryos were electroporated with mouse 5 kb EGFP, marmoset 5 kb EGFP, or marmoset 10 kb EGFP vectors together with a mCherry reporter vector under the control of a ubiquitous promoter. The electroporated areas were identified by the mCherry reporter expression. DP and VP territories were targeted at E11.5 and analyzed at E14.5 (C-F).

(C) Examples of EGFP⁺ cells (red arrowheads) in the VZ/SVZ and postmitotic compartment of marmoset 5 kb EGFP (n = 3) and marmoset 10 kb EGFP electroporated samples (n = 4). No EGFP is detected in electroporated embryos using mouse 5 kb EGFP (n = 3). High magnifications of yellow-dashed boxes are shown on the right. mCherry⁺EGFP⁺ neurons in postmitotic compartment are indicated by red arrowheads. The mouse 5 kb EGFP panel shows only nonspecific background fluorescence. Note that despite of large targeted mCherry⁺ domains, no EGFP expression was observed in the subpallium.

(D) EGFP immunofluorescence and mCherry fluorescence in the DP. Examples of mCherry⁺EGFP⁺ cells in CP + IZ and VZ + SVZ are indicated with red arrowheads.

(E) Percentage of EGFP⁺ cells in the CP + IZ and VZ + SVZ among the total mCherry⁺ electroporated cells in the DP upon electroporation with mouse 5 kb EGFP (n = 3, black circles), marmoset 5 kb EGFP (n = 3, gray circles), and marmoset 10 kb EGFP (n = 5, blue circles). Data are from different electroporated embryos and litters (n = 3); the total number of counted mCherry⁺ and EGFP⁺ cells for mouse 5 kb (463 and 2), CP + IZ (253 and 0), and VZ + SVZ (210 and 2); marmoset 5 kb (570 and 47), CP + IZ (292 and 9), and VZ + SVZ (278 and 38); and marmoset 10 kb (1356 and 212), CP + IZ (936 and 90), and VZ + SVZ (420 and 122); ***p < 0.001, **p < 0.01; one-way ANOVA; error bars indicate SEM.

(F) Immunofluorescence for EGFP and *Nurr1* or *Ctip2*. Examples of EGFP⁺ cells of marmoset 10 kb EGFP electroporated samples in the DP. High magnifications of yellow-dashed boxes are shown on the right. EGFP⁺*Nurr1*⁺ and EGFP⁺*Ctip2*⁺ neurons in postmitotic compartment are indicated by yellow arrowheads.

DP, dorsal pallium; CP, cortical plate; IZ, intermediate zone.

Scale bars represent 50 μ m (C, D, and F) and 10 μ m (high magnifications in C and F).

EGFP reporter constructs driven by either a well-conserved mammalian region alone (5 kb mouse or 5 kb marmoset proximal elements) or together with the primate-specific region (10 kb marmoset) by *ex vivo* electroporation (Figure 2B). We first electroporated the constructs at E12.5, corresponding to the peak of *Dbx1* expression in the mouse, and analyzed embryos

24 h later (Figures S2A and S2B). The mouse 5 kb elements drove EGFP expression in a restricted number of cells at the VP, although a larger region was electroporated, as labeled by mCherry expression under the control of a ubiquitous promoter (Figure S2B), recapitulating the expected expression of mouse *Dbx1* (Figure S1G). Compared to the mouse, the two marmoset

constructs promoted enhanced EGFP expression in the mitotic compartment of the VP (Figure S2B). To test whether the primate elements were capable to promote expression also in the post-mitotic compartment, as expected by the human expression data, we electroporated at E11.5, a stage when *Dbx1* is first expressed in the VP/PSB, and analyzed 3 days later at E14.5, corresponding to a time when *Dbx1* expression is low (Figure S1G). As expected, we detected almost no EGFP expression driven by the mouse 5 kb elements in both VZ/SVZ and neurons (Figure 2C). In contrast, the marmoset 5 kb elements were active in progenitors and neurons in the VP, and the 10 kb elements showed a stronger activity in both (Figure 2C). Furthermore, we observed EGFP⁺ cells in both mitotic and postmitotic compartments of the DP (Figures 2D and 2F; see STAR Methods), suggesting that the primate-specific elements are capable to promote an ectopic expression in neocortical progenitors and neurons. We thus quantified the percentage of ectopically induced EGFP⁺ cells in the DP (Figures 2D and 2E). While we observed almost no EGFP expression driven by the mouse 5 kb elements in both VZ/SVZ ($0.95\% \pm 1.3\%$) and neurons in the CP and the intermediate zone (IZ) (0%) (Figure 2D and black circles in Figure 2E), the marmoset 5 kb elements promoted EGFP expression in cells in the VZ/SVZ ($13.7\% \pm 2.1\%$) and CP/IZ ($3.1\% \pm 1.6\%$) (Figure 2D and gray circles in Figure 2E). The 10 kb elements showed a strong induction of EGFP⁺ cells in the VZ/SVZ ($29.0\% \pm 3.3\%$) and CP/IZ ($9.6\% \pm 1.3\%$) compared to both mouse and marmoset 5 kb elements (Figure 2D and blue circles in Figure 2E). We further characterized the identity of the cells expressing the reporter EGFP driven by the 10 kb elements in the DP and VP postmitotic compartment at E14.5. In the DP, we observed EGFP⁺ cells co-expressing *Ctip2* (Figure 2F), a marker for early-born neurons (Molyneux et al., 2007), and *Nurr1* (Figure 2F), a marker for SP neurons (Hoerder-Suabedissen and Molnár, 2013). Moreover, in the VP, strongly labeled EGFP⁺ cells co-expressed CP, CR, and SP neuronal markers such as *Tuj1*, *Ctip2*, *Tbr1*, *Reln*, *Calr*, and *Nurr1*, confirming high EGFP expression in neurons (data not shown). This strong EGFP neuronal expression could, however, reflect either EGFP protein stability (its half-life normally being 26 h; Corish and Tyler-Smith, 1999) or 10 kb promoter activity in newly-born neurons. To discriminate between these two possibilities, we electroporated the 10 kb construct at E11.5 and performed 5-Ethynyl-2'-deoxyuridine (EdU)-birthdating analysis by pulse labeling at E12.5 and embryo collection at E14.5 (Figure S3). We observed high EGFP expression in (1) EdU⁻mCherry^{high} neurons born before the EdU administration (NL1), (2) EdU⁺mCherry⁺ neurons born at E12.5 (NL2), and (3) EdU⁻mCherry⁻ neurons (NL3) born from progenitors, which underwent several rounds of divisions. This argues in favor of the primate-specific elements being transcriptionally active also in neurons.

To ensure that the activity of the 10 kb elements was not due to its episomal expression, we generated *marmoset 10kb::EGFP* transgenic mice and analyzed EGFP expression pattern at E12.5 embryos. While *Dbx1*⁺EGFP⁺ cells were restricted to the mitotic compartment in the VP (Figures 3A and 3B, yellow arrowheads), *Dbx1*⁻EGFP⁺ cells were also observed in the mitotic and postmitotic compartments of the VP and of the DP (Figures 3A–3C). Ectopic EGFP expression in progenitors and neurons in the

DP was confirmed in three additional *marmoset 10kb::EGFP* transgenic mouse lines (Figure 3D). The percentage of EGFP⁺*Ctip2*⁺ neurons and EGFP⁺*Ctip2*⁻ progenitors was similar within different transgenic mouse lines (Figure 3E), confirming that ectopic EGFP expression in progenitors and neurons in the DP was induced due to the activity of the marmoset 10 kb elements irrespective of the transgene insertion sites. Expression of the transgene was also detected in the postmitotic compartment in other regions of the CNS where *Dbx1* is normally expressed in progenitors in the mouse such as in the thalamus, midbrain, hindbrain, and spinal cord (Figures 3A, 3D, and S4). Together, the activity of the primate-specific elements analyzed using electroporation and transgenic animals is consistent with the endogenous *Dbx1* expression pattern in primate embryos and argues in favor of the identified genomic sequences corresponding to *cis*-regulatory elements of the *Dbx1* gene in primates.

Ectopic *Dbx1* Expression in Mouse Pallial Progenitors and Neurons Induces CR and SP Neuron Fate

To address the effect of the evolutionary gain of *Dbx1* expression in DP territory, we examined the phenotype induced by *Dbx1* overexpression in DP progenitors by *ex*-*in utero* electroporation at E11.5 (Figure 4A). As *Dbx1* progenitors in the VP were shown to give rise to CR neurons in the mouse cerebral cortex (Bielle et al., 2005), we first examined CR markers 48 h after electroporation and detected significantly higher numbers of *Reln*⁺ neurons (~16.5%) among *Dbx1* transfected cells (pCAGGS-*Dbx1*-iresGFP) compared to control (pCAGGS-iresGFP) (Figures 4B–4D). We also analyzed the expression of *Calr*, another marker of CR neurons as well as of SP neurons at early stages (Pedraza et al., 2014; Fonseca et al., 1995), and cortical interneurons at later stages (Gelman and Marín, 2010). While the *Reln*⁺ neurons were either *Calr*⁺ or *Calr*⁻ (~8.9% EGFP⁺*Calr*⁺*Reln*⁺ and ~7.6% EGFP⁺*Calr*⁻*Reln*⁺), ~18.2% of *Calr*⁺ neurons were *Reln*⁻ (Figures 4C and 4D). We observed no induction of the interneuron marker (GABA) upon *Dbx1* overexpression (Figures S5A and S5B), whereas we detected a precocious induction of *Nurr1*, a gene normally expressed in SP neurons at later stages of development (~E15) (Hoerder-Suabedissen and Molnár, 2013) (Figures 4E–4G; ~24% *Nurr1*⁺*Calr*⁻ and ~10% *Nurr1*⁺*Calr*⁺) and thus not expressed at E13.5 in the DP (Figure 4E, control EGFP panels). This suggests that *Dbx1* overexpression induces ectopic CR neurons generation and precocious SP-like identity. Importantly, upon *Dbx1* ectopic expression, we observed *Calr*⁺ axons extending laterally (Figure 4E, red arrowheads), characteristic of preplate neurons, which occupy the SP zone at later stages of development (De Carlos and O'Leary, 1992; McConnell et al., 1989). Together, these results also show that *Dbx1* ectopic expression in the DP induces both early and late SP markers simultaneously.

Dbx1 is unlikely to be involved in the generation of SP neurons in mice, as we rarely observed *Dbx1*-derived progeny expressing *Nurr1* using permanent tracing (Figure S5C), and is exclusively restricted to the lateral cortex. We further examined whether such ectopically generated *Nurr1*⁺EGFP⁺ neurons had characteristics of mouse SP neurons as at later stages of development, namely glutamatergic identity based on *Ctip2* (McKenna et al., 2011) and/or *Tbr1* expression (Hevner et al.,

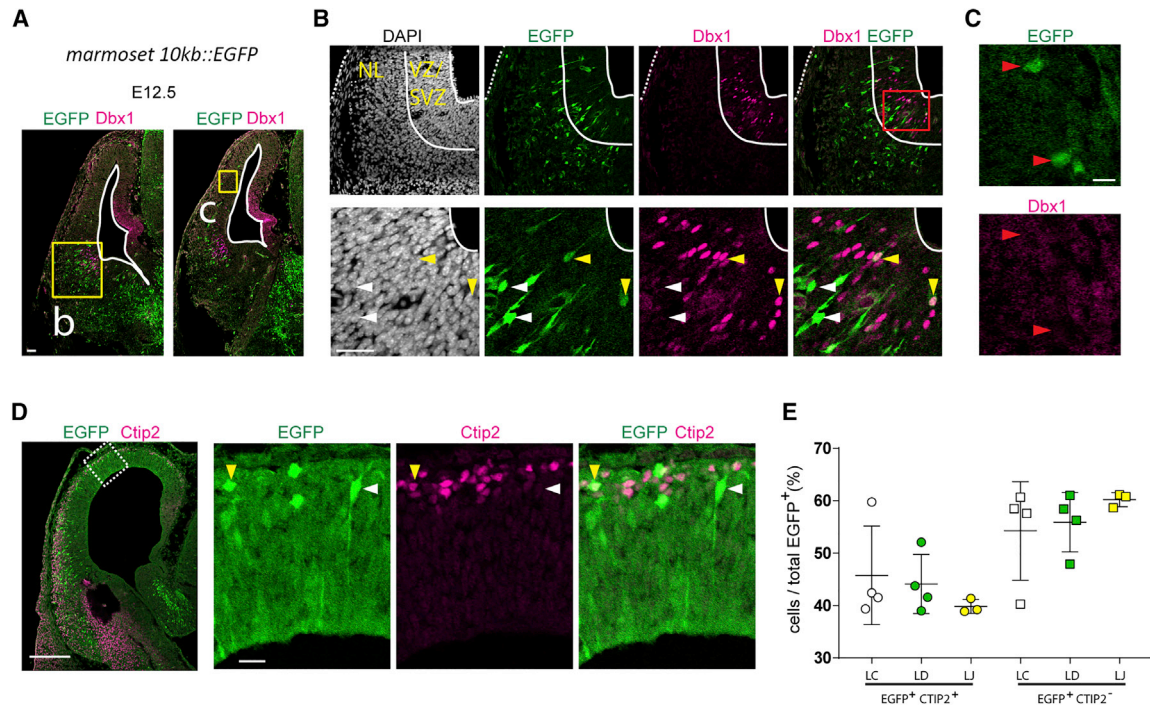


Figure 3. DP Ectopic Expression in *marmoset 10 kb-EGFP* Transgenic Lines

(A) EGFP and Dbx1 immunofluorescence using *marmoset 10kb::EGFP* transgenic mice at E12.5. GFP⁺ cells are also found in the postmitotic compartment of the thalamus, where Dbx1 is normally expressed in progenitor cells in the mouse.

(B) Examples of Dbx1⁺EGFP⁺ and Dbx1⁻EGFP⁺ cells both in the VZ/SVZ and postmitotic compartment at the VP (n = 5 from two different litters). High magnification of the red box is shown in bottom panels. In the VZ/SVZ, Dbx1⁺EGFP⁺ and Dbx1⁻EGFP⁺ cells are shown by yellow and white arrowheads, respectively.

(C) Examples of Dbx1⁻EGFP⁺ cells in the DP close to the postmitotic compartment.

(D) EGFP and Ctip2 immunofluorescence using *marmoset 10kb::EGFP* transgenic mice at E12.5. High magnification of the white-dashed box is shown on right panels. Examples of EGFP⁺Ctip2⁺ neurons (yellow arrowheads) and EGFP⁺Ctip2⁻ (white arrowheads) in the DP.

(E) Percentage of EGFP⁺Ctip2⁺ neurons and EGFP⁺Ctip2⁻ progenitors in the DP. The number of counted EGFP⁺Ctip2⁺ (round dots) and EGFP⁺Ctip2⁻ (square) cells from three different transgenic mouse lines (n = 4 embryos for C [LC] and D [LD] transgenic lines and n = 3 embryos for transgenic J line [LJ]) marked as the black, green, and yellow are LC, 181 and 231; LD, 865 and 1,115; and LJ, 152 and 228, respectively. None of the data pairs are statistically significant (one-way ANOVA); error bars indicate SD.

Scale bars represent 100 μ m (A and D, left panel), 50 μ m (B and D, right panels), and 10 μ m (C).

2001), position in the SP, and axonal projection to the internal capsule (IC) and the corpus callosum (CC) through the IZ (Hoerder-Suabedissen and Molnár, 2015). While we observed Nurr1⁺Tbr1⁺EGFP⁺ and Nurr1⁺Ctip2⁺EGFP⁺ neurons in the SP (Figures 4H, S5D, and S5E), the vast majority of Nurr1⁺EGFP⁺ neurons were located in the IZ (Figures 4H, 4I, and S5F). Nurr1⁺EGFP⁺ neurons in the IZ were either Tbr1⁺ or Tbr1⁻ (Figure 4H, blue and red arrowheads, respectively) but mostly Tbr1⁺ in the CP, suggesting that EGFP⁺Tbr1⁻ represented neurons not having finished their migration. Ectopic Nurr1⁺ neurons induced by Dbx1 overexpression retained Nurr1 expression whether they were localized in the SP, IZ, or CP, suggesting that Dbx1 maintenance prevents them to become deep-layer neurons. This argued against these Dbx1-induced Nurr1⁺Ctip2⁺ neurons being “en passant” cortical plate neurons, as suggested in hPSC cultures (Ozair et al., 2018). Moreover, EGFP⁺ neurons appeared to extend projections toward the prospective CC and the IC (Figures 4I–4K, red arrowheads), suggesting that Dbx1 overexpression induced molecularly distinct SP-like neu-

rons. We then wonder whether such a neuronal population co-expressing Dbx1 and SP markers was present in human embryos. We identified Dbx1⁺Nurr1⁺Ctip2⁺ neurons (Figures S5G–S5I) in a ventral region of the cortex of a human embryo at CS18–CS19/GW6.5, indicating that a population with similar molecular identity might exist in the developing human. While we did not detect this population in the SP or DP territories at the age we analyzed, Dbx1 expression in the pallial SP was observed in human fetuses (BrainSpan, 2011) at later developmental stages (<http://brainspan.org/lcm/gene/78785>), consistent with our data. These results strongly support the conclusion that Dbx1 ectopic expression in the mouse induces a SP fate and suggest the possibility that Dbx1-expressing SP neurons exist in the DP in human embryos.

Restricted Dbx1 Expression in Neurons Induces Exclusively a SP Fate

The critical step of neuronal fate decision is thought to occur at the progenitor level, followed by the subsequent maturation of

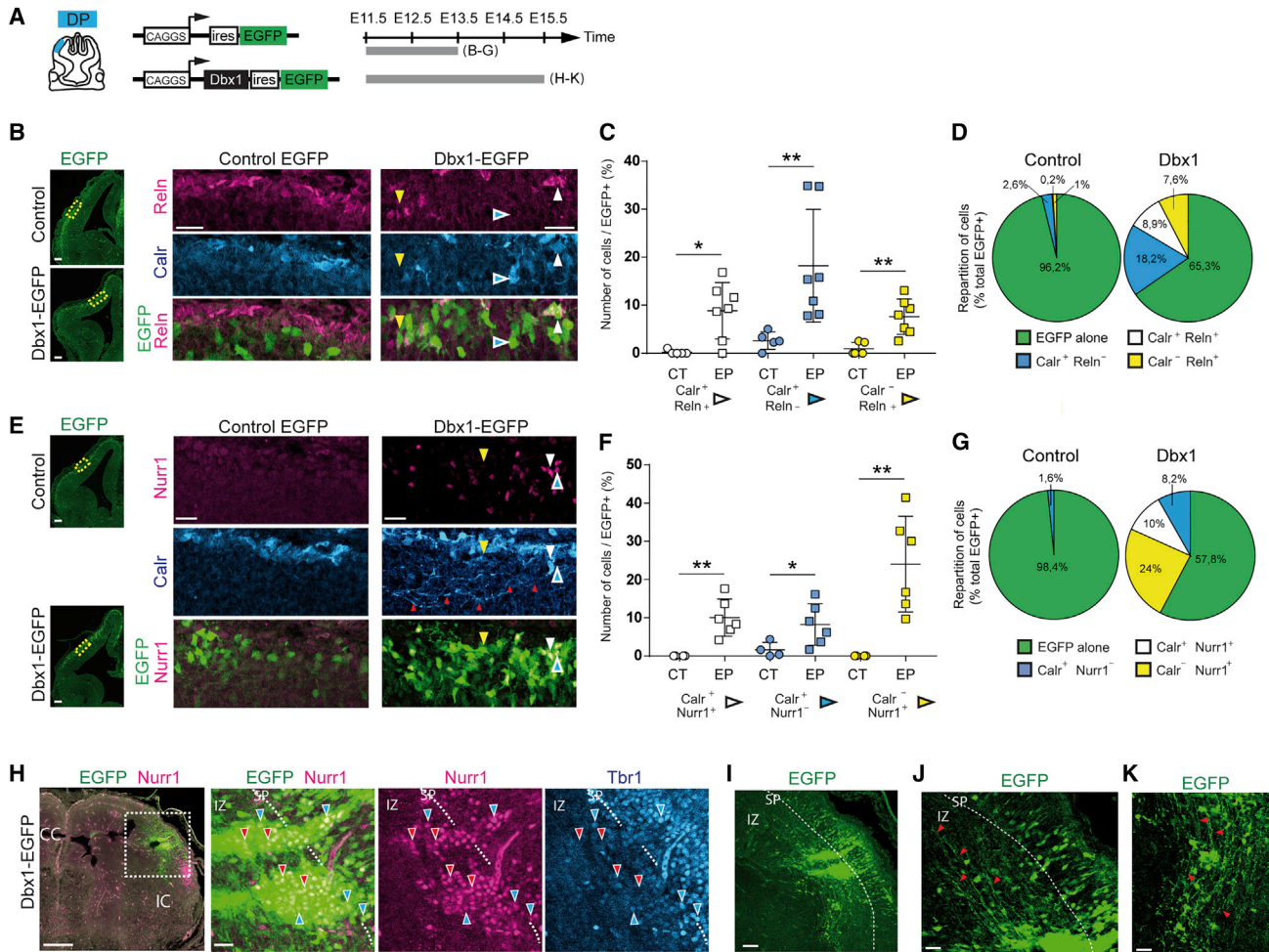


Figure 4. Dbx1 Overexpression Promotes Ectopic Generation of CR and SP Neurons

(A) Experimental design: wild-type mouse developing cortices were electroporated with either control pCAGGS-ires-EGFP or pCAGGS-Dbx1-ires-EGFP. (B–K) The DP of embryos was targeted at E11.5 and analyzed at E13.5 (B–G) or E15.5 (H–K). The left side of each panel (B and E) is the direction of the internal capsule.

(B) EGFP, Reln, and Calr immunofluorescence. High magnifications of yellow-dashed boxes are shown in right panels. Examples of EGFP⁺Calr⁺Reln⁺ (white arrowheads), EGFP⁺Calr⁺Reln⁻ (blue arrowheads outlined in white), and EGFP⁺Calr⁻Reln⁺ (yellow arrowheads) neurons.

(C) Quantifications of EGFP⁺Calr⁺Reln⁺ (white), EGFP⁺Calr⁺Reln⁻ (blue), and EGFP⁺Calr⁻Reln⁺ (yellow) neurons in the ires-EGFP control (CT) and Dbx1-EGFP electroporated embryos (EP). Data show the percentage of induced cells from each 11 (CT) and 28 (EP) fields from six different embryos and litters (n = 6); error bars indicate SD. Total number of EGFP⁺ cells analyzed: CT, 486; EP, 1,221; *p < 0.05, **p < 0.01, ***p < 0.001; unpaired t test, two tailed. Note that the three ectopically induced neuronal populations in the EP group (EGFP⁺Calr⁺Reln⁺, EGFP⁺Calr⁺Reln⁻, and EGFP⁺Calr⁻Reln⁺) are statistically different when analyzed by one-way ANOVA; **p < 0.01.

(D) Repartition of cells expressing EGFP alone or in combination with Calr and Reln among EGFP electroporated cells in (B).

(E) EGFP, Nurr1, and Calr immunofluorescence. High magnifications of yellow-dashed boxes are shown in right panels. Examples of EGFP⁺Nurr1⁺Calr⁺ (white arrowheads), EGFP⁺Nurr1⁺Calr⁻ (blue arrowheads outlined in white), and EGFP⁺Nurr1⁻Calr⁺ (yellow arrowheads) neurons. Calr⁺ axons projecting toward the IC were observed upon Dbx1-EGFP overexpression (red arrowheads).

(F) Quantifications of EGFP⁺Nurr1⁺Calr⁺ (white), EGFP⁺Nurr1⁺Calr⁻ (blue), and EGFP⁺Nurr1⁻Calr⁺ (yellow) neurons in CT and EP embryos. Data shows the percentage of induced cells from 10 (CT) and 30 (EP) fields from different embryos (CT n = 5, EP n = 6) and litters. Total number of EGFP⁺ cells analyzed: CT, 393; EP, 1,499; error bars indicate SD; ***p < 0.001; unpaired t test; two tailed. Note that the three ectopically induced neuronal populations in the EP group (EGFP⁺Nurr1⁺Calr⁺, EGFP⁺Nurr1⁺Calr⁻, and EGFP⁺Nurr1⁻Calr⁺) are statistically different when analyzed by one-way ANOVA; ***p < 0.001.

(G) Repartition of cells expressing EGFP alone or in combination with Calr and Reln among EGFP electroporated cells in (E).

(H) EGFP, Nurr1, and Tbr1 immunofluorescence. High magnifications of the white-dashed box are shown on the right panels. Examples of EGFP⁺Nurr1⁺Tbr1⁺ (blue arrowheads outlined in white) and EGFP⁺Nurr1⁺Tbr1⁻ (red arrowheads outlined in white) neurons (n = 3). In the IZ 23% of EGFP⁺Nurr1⁺ neurons coexpress Tbr1 while almost all when the electroporated cells reached the CP.

(I–K) EGFP⁺ neurons project their axons toward the CC (I and J [high magnification]) and the IC (I and K [high magnification]) indicated by red arrowheads. CC, corpus callosum; IC, internal capsule.

Scale bars, 50 μ m (B, E, and I), 300 μ m (H), 25 μ m (J and K; high magnification in B, E, and H).

a fate-committed neuron (Greig et al., 2013). We therefore asked whether the maintenance of Dbx1 expression in neurons as observed in primates displayed specific functions. To address this question, we targeted Dbx1 expression solely to neurons by using a *Cre-loxP* recombination system (Figure 5A) to induce Dbx1 in NEX-expressing cells, a neuronal basic helix-loop-helix protein expressed only in postmitotic cells (Wu et al., 2005; Goebbels et al., 2006; Chou et al., 2009; Alfano et al., 2014; Golonzhka et al., 2015; Kazdoba et al., 2012). We verified that the Cre and Dbx1 proteins were specifically expressed in postmitotic Tuj1⁺ cells (Figure S6). We found that postmitotic Dbx1 was unable to induce Reln⁺ (2.0% ± 1.1%) and Calr⁺ (2.2% ± 1.3%) in the DP (Figures 5B and 5D), suggesting that Dbx1 activity is required in progenitors to generate CR and Calr⁺ neurons. Dbx1 postmitotic expression was compatible with Ctip2 expression and was capable of inducing the ectopic expression of Nurr1 (40.9% ± 1%) (Figures 5C and 5D). Taken together, our results showed that specific Dbx1 expression in neurons is sufficient to change cell identity and impart an SP-like neuron fate and further argue in favor that the acquisition of a postmitotic Dbx1 expression in the primate dorsal cerebral cortex could have led to the generation of a novel subtype of SP neurons expressing Nurr1 and Dbx1, a molecular signature not observed in the mouse.

DISCUSSION

Our work combines evolutionary and developmental approaches to elucidate a novel pathway that may have driven the expansion of pioneering CR and SP neurons during cortical evolution in primates through the role of primate-specific genomic elements of a single cell-fate determinant, the Dbx1 gene.

Both mutations directly affecting coding sequences and gene regulatory elements are thought to have participated in evolutionary changes (King and Wilson, 1975; Siepel and Arbiza, 2014; Boyd et al., 2015; Khaitovich et al., 2006). We identified a genomic sequence spanning –10 to –5 kb upstream of the *Dbx1* transcription start site, which is specifically conserved in primates. A homologous genomic sequence exists in the mouse genome but on another chromosome (G. D’Onofrio, data not shown). It is thus likely that this genomic sequence was inserted in the primate lineage upstream of the –5 kb regulatory elements conserved in all mammals. In the mouse the primate-specific sequence drives the expression of a reporter gene in the VP, mimicking the endogenous Dbx1 expression, but also in the DP and lateral pallium (LP), where *Dbx1* is not expressed. Moreover, despite the large region targeted with electroporation, which also included the lateral ganglionic eminence (LGE) in the subpallium, no EGFP expression was detected in LGE progenitors. Together, this showed that the sequence identified is a *cis*-regulatory region, which could respond positively to factors present in the DP and LP, but absent from the LGE, or negatively to a repressor factor present in the LGE. Regulatory factors binding to this element could also either activate directly Dbx1 expression in the DP and LP or relieve a repression in the DP and LP, both ultimately resulting in the expansion of the Dbx1-expressing territory but through distinct transcription regulatory

mechanisms. Interestingly, intact –5 kb mouse regulatory sequences are essential to ensure the proper restriction of Dbx1 in the VP. Indeed, when a 3.2 kb sequence located 2.7 kb upstream of the first murine Dbx1 exon fused to the Hsp68 minimal promoter was used to trace Dbx1 derivatives by *in utero* electroporation (IUE), GFP-positive cells were found in the VZ of the DP (Rueda-Alaña et al., 2018), a situation that is never encountered using genetic tracing with the *Dbx1*^{CRE} mouse line (knockin of CRE into the 3′ UTR of the *Dbx1* gene) (Bielle et al., 2005; Griveau et al., 2010; Teissier et al., 2010) or when the mouse 5 kb sequence is used to drive GFP expression.

In the chick and mouse, spinal cord Dbx1 expression was shown to be restricted to the intermediate region spanning the alar-basal plate boundary by tight repression dependent on dorsal and ventral signals from patterning centers and cross-repressing interactions between progenitor fate determinants (Pierani et al., 2001, 1999; Briscoe et al., 2000). In the telencephalon, Dbx1 expression is also very stringently controlled both in time and space and is found altered in many mouse mutants for genes involved in patterning of the early pallium such as Pax6, Lhx2, Gsh2, Tlx, Pbx, Dmrt5, and Gli3 (Golonzhka et al., 2015; Stenman et al., 2003; Friedrichs et al., 2008; Mangale et al., 2008; Carney et al., 2009; Cocas et al., 2011; Saulnier et al., 2013; Yun et al., 2001). Most of these genes function to restrict Dbx1 expression in progenitors at the VP. This suggests that inhibition of its expression is a converging point of multiple pathways possibly through a common repressor(s). This also highlights the high sensitivity of the Dbx1 regulatory sequences to different single gene deletions and, thus, the high plasticity of its transcriptional control providing a favorable ground for evolutionary changes. Evolutionary changes of expression pattern and/or levels of factors mediating cortical patterning may participate in the expansion of Dbx1 expression as we observed in a human fetus.

What could be the meaning of an expansion of the territory expressing Dbx1? In the murine neocortex, Dbx1 expression is highly restricted both spatially and temporally to the VP progenitor domain (Bielle et al., 2005; Puelles and Rubenstein, 1993; Teissier et al., 2010). The expanded Dbx1⁺ domain in the human embryo suggests that either its expression was newly recruited in the DP compartment or that an enlargement of the VP domain occurred in humans. Since the acquisition of Dbx1 expression in the VP has been shown to occur in mammals (Bielle et al., 2005), it is possible that the expansion of the VP in humans reflects the progressive acquisition and continuous evolutionary expansion of the Dbx1-expressing VP domain. The relevance of the VP widening during cortical evolution has been hypothesized to contribute to the enlargement of the neocortex (Borello and Pierani, 2010; Karten, 1997; Molnár and Butler, 2002; Puelles, 2011), including the ventral part of the DP and the amygdala, by supplying VP-derived excitatory neurons (Puelles, 2011). Indeed, in mouse, Dbx1-derived excitatory neurons, namely CRs and cortical plate transient neurons (CPTs), are generated from VP progenitors and migrate to the DP cortical plate (Bielle et al., 2005; Teissier et al., 2010) and amygdala (Hirata et al., 2009; Waclaw et al., 2010). In favor of the proposed VP expansion hypothesis, the evolutionary appearance of Dbx1-expressing VP domain could thus participate to neocortical evolution in

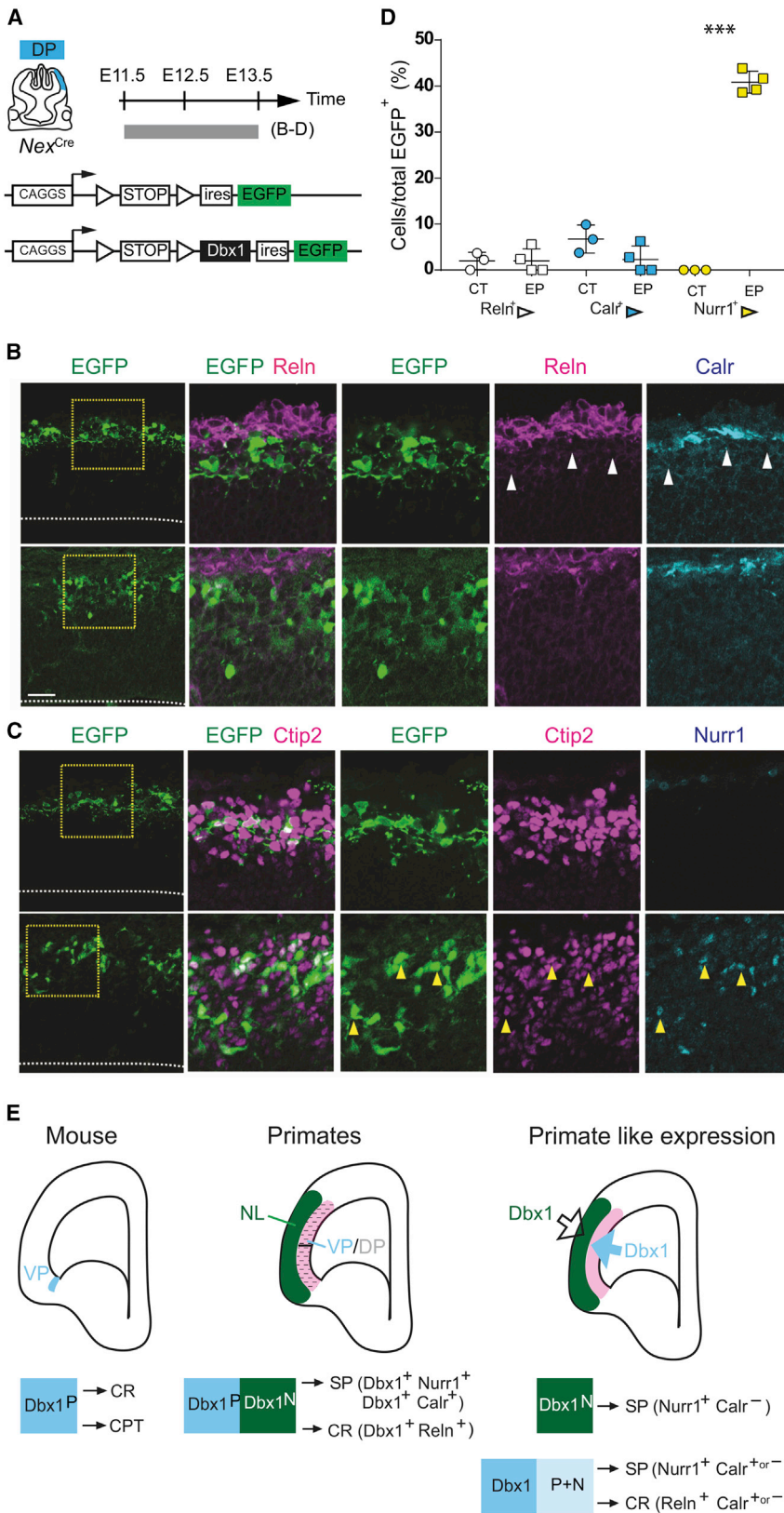


Figure 5. Specific Dbx1 Overexpression in Neurons Induces Nurr1 Expression

(A) Experimental design: *Nex^{Cre}* mouse embryos were electroporated with pCAGGS-ires-EGFP or pCAGGS-loxP-stop-loxP-Dbx1-ires-EGFP plasmids. The DP of embryos were targeted at E11.5 and analyzed at E13.5 (B–D).

(B and C) Immunofluorescence for EGFP, Reln, and Calr (B) and for EGFP, Ctip2, and Nurr1 (C). High magnifications of yellow-dashed boxes in right panels show no induction of Reln or Calr (white arrows) (B), a co-labeling with Ctip2, and an induction of Nurr1 (yellow arrows) (C). White-dotted lines indicate the VZ.

(D) Percentage of Reln⁺ (white), Calr⁺ (blue) and Nurr1⁺ (yellow) cells within EGFP⁺ electroporated cells in the DP upon electroporation with control pCAGGS-ires-EGFP (CT) or pCAGGS-loxP-stop-loxP-Dbx1-ires-EGFP (EP) plasmids. Data show the percent of EGFP cells from one or two sections from different embryos (CT n = 3, EP n = 4). Total number of counted EGFP⁺ cells analyzed: CT, 461; EP, 438. Error bars indicate SEM; ***p < 0.001; one-way ANOVA and Tukey's multiple comparison test.

(E) Summary of evolutionary changes of Dbx1 expression and cell identities in wild-type and Dbx1-overexpressing mouse embryos. Dbx1 expression domains in mouse and primate embryos. The same shape of the brain is utilized for simplicity. While Dbx1 expression is restricted to progenitor cells (Dbx1^P) at the VP in the mouse, in primates, it is newly acquired in the postmitotic compartment (Dbx1^N) (green), and in human, it is extended dorsally in the proliferative SVZ (dotted pink). Expansion to the SVZ is not detected in the macaque samples analyzed here, and the expansion in the human SVZ could represent an extended VP or an enlarged expression in the DP. Primate-specific cis-elements promote reporter expression in VP/DP progenitors and neurons. In the mouse, Dbx1 is expressed in VP progenitors giving rise to CR and CPT neurons, and in primates, it is expressed in neurons co-expressing Reln and/or Calr or Nurr1, representing CR subtypes and possibly SP neurons, respectively. Dbx1 overexpression in DP progenitors and neurons, mimicking the expression of primates in the mouse developing cortex, promotes CR (Reln⁺ and/or Calr⁺) and SP neuron identity (Nurr1⁺ and/or Calr⁺). SP fate (Nurr1⁺Calr⁻) is also induced by Dbx1 expression exclusively in neurons. Whether Nurr1⁺Calr⁺ and Nurr1⁺Calr⁻ cells represent molecularly distinct SP subtypes, similarly to what has been shown in mice for CRs, has yet to be determined.

VP, ventral pallidum; NL, neuronal layer. SP, subplate zone; IZ, intermediate zone; CC, corpus callosum; IC, internal capsule.

Scale bars, 50 μ m (B and C), 25 μ m (high magnifications in B and C).

particular via an increase of excitatory CR and SP neurons in DP cortical layers (Arai and Pierani, 2014; Hoerder-Suabedissen and Molnár, 2015; Puellas, 2011; Smart et al., 2002). However, we did not detect an expansion of Dbx1-expressing progenitors in the limited macaque sections and stages that we were able to analyze, suggesting that either this expression is still highly spatially and/or temporally restricted to specific regions and stages or it is a human-specific feature.

Notably, in both macaque and human fetuses, we observed postmitotic *Dbx1* expression and, consistently, primate-specific sequences drove sustained expression not only in progenitors but also in neurons, unlike the *Dbx1* mammalian conserved upstream regulatory sequences that induced reporter expression exclusively in VP progenitors. Although still restricted to specific domains, *Dbx1* expression in neurons is also observed in other regions of the developing human nervous system, such as the hindbrain and spinal cord, arguing for a more general shift in enhancer activity. As for the expression in progenitors, it is still an open question whether the primate-specific regulatory sequences could mediate derepression in neurons rather than activation. The primate -10 to -5 sequence seems therefore to regulate two key aspects of *Dbx1* expression, its spatial and cell type-specific regulation, two levels of transcriptional control that might represent critical evolutionary advancements underlying the increase in number and diversity of neuronal subtypes in the cerebral cortex, particularly pioneer neurons of the preplate.

As to the functional relevance of evolutionary changes in *Dbx1*-expressing territories, previous reports have shown that *Dbx1* is a potent determinant of neuronal identity in the spinal cord (Pierani et al., 2001), rhombencephalon (Bouvier et al., 2010), and diencephalon (Sokolowski et al., 2015). In the developing spinal cord, progenitors expressing *Dbx1* generate V0 interneurons and the ectopic induction of *Dbx1* in neighboring progenitor domains induces V0 and represses V1 interneurons, showing that *Dbx1* is a V0 fate determinant (Pierani et al., 2001). In the mouse cerebral cortex, *Dbx1* is expressed in cortical progenitors at the VP, which give rise to CR neurons (Bielle et al., 2005). We show here that upon the ectopic induction of *Dbx1* in the DP, the CR marker *Reln* was induced. This result is in agreement with previous observations showing that in the quail, *Dbx1* ectopic expression induced *Reln* (Nomura et al., 2008). In the mouse pallium, *Dbx1* thus also behaves as a fate determinant of CR neurons when expressed in progenitor cells. Unexpectedly, the expression of *Dbx1* in DP and LP progenitors also induced *Calr*⁺*Reln*⁻, a signature of early-born preplate neurons (Fonseca et al., 1995; García-Moreno et al., 2007), including SP neurons (Pedraza et al., 2014) but also interneurons at later stages (Gelman and Marín, 2010). At the developmental stage we analyzed (between E11.5 and E13.5), *Calr*⁻ and *Calr*⁺ SP neurons are generated from progenitors in the DP (Pedraza et al., 2014), some of which turn on *Nurr1* expression later (~E15.5; Hoerder-Suabedissen and Molnár, 2013). Upon *Dbx1* misexpression, the observed precocious induction of *Nurr1* in cells located in the SP and cortico-fugal axonal projections, together with the absence of the interneuron marker GABA, strongly argues in favor of *Dbx1* promoting also SP-like identities. The postmitotic activity of *Dbx1* in promoting *Nurr1* expression, but not that of *Reln*, shows that the induction of SP-like

identities does not depend on a progenitor function of *Dbx1*. The generation of CR and SP neurons could thus reflect distinct *Dbx1* activities depending on the mitotic or postmitotic status of the cell. These results strongly suggest that *Dbx1* is capable of reprogramming committed neurons to a distinct fate, including their differentiated features in terms of final location upon migration, molecular expression profile, and axonal projections. This is consistent with the *Dbx1* function demonstrated in progenitors in other regions of the developing CNS and shows for the first time that in the cerebral cortex, *Dbx1* can likely control a full transcriptional program responsible for neuronal identity in postmitotic cells.

Neuronal identity is established sequentially from progenitors to young neurons through progressive fate restriction and acquisition of specific combination of transcription factor expression (Schuurmans and Guillemot, 2002; Shirasaki and Pfaff, 2002; Briscoe and Novitsch, 2008). In the cerebral cortex, a period of fate plasticity in young neurons exists during which transcription factors later on restricted to different subtypes are coexpressed (Greig et al., 2013). This is generally mediated by cross-repressive interactions between postmitotic cell fate determinants (Chen et al., 2008; De la Rossa et al., 2013; Srinivasan et al., 2012). However, as in the case of *Tbr1*, a feedback control on patterning centers was also observed, leaving open the possibility that some of the cell fate changes depend on patterning centers and thus through an intermediate progenitor state (Elsen et al., 2013; Bedogni et al., 2010). Very recent studies discriminated the postmitotic role of transcription factors (TFs) expressed in both progenitors and neurons using similar genetic tools based on *Nex:Cre* expression (Wu et al., 2005; Alfano et al., 2014; Golonzhka et al., 2015; Zembrzycki et al., 2015; Kazdoba et al., 2012; Fame et al., 2016; Nakamura et al., 2016) in controlling area-specific properties and laminar fate. Together, these reports (Arlotta and Hobert, 2015; De la Rossa et al., 2013) and our work underlie the rising concept of the key role of TFs expressed in postmitotic neurons as potent cell fate determinants. Our data unravel for the first time a putative mechanism mediating preplate identity and in particular CR versus SP fate. They identify a role for *Dbx1* as a fate determinant in SP-like fate possibly linked to its postmitotic expression characteristic of primates. Lastly, our results reveal an unexpected degree of plasticity in fate determination in particular for *Nurr1*⁺ SP neurons. *Dbx1* expression in progenitors or neurons induces molecularly distinct SP neurons (Figure 5E), suggesting that *Dbx1* can impart subtype-specific SP identity depending on its temporal and spatial regulation of expression. SP neurons are well known as “hub neurons” that mediate afferent and efferent cortical pathfinding and also promote intra-cortical and extra-cortical circuitries (Kanold and Luhmann, 2010). They are present transiently during development and disappear early in postnatal life in mice (Price et al., 1997). *Nurr1*⁺ SP neurons are born between E11.5 and E12.5 in mice and have been described to preferentially survive during the first postnatal weeks (Hoerder-Suabedissen and Molnár, 2013), when SP neurons receive inputs from cortical layers (Viswanathan et al., 2012). A pronounced increase in the number of SP neurons and complexity of cortical circuits has been observed in primates compared to other mammals (Hoerder-

Suabedissen and Molnár, 2015; Smart et al., 2002). It is therefore tempting to speculate that the presence of Nurr1⁺Dbx1⁺ SP neurons in humans may have contributed to the expansion of the SP neuron pool, in particular a subpopulation with specific survival characteristics, which could affect the period of cortical projection formation.

STAR★METHODS

Detailed methods are provided in the online version of this paper and include the following:

- KEY RESOURCES TABLE
- LEAD CONTACT AND MATERIALS AVAILABILITY
- EXPERIMENTAL MODEL AND SUBJECT DETAILS
 - Animals
- METHOD DETAILS
 - Immunofluorescence
 - *In situ* hybridization
 - Exo-in utero electroporation
 - EdU pulse labeling and staining
 - Cloning of marmoset 5 and 10kb genomic DNA sequences
 - Generation of 10kb marmoset transgenic mice
 - Cloning of Dbx1 overexpression and Cre-inducible expression vectors
 - Multiple alignments of genomic sequences upstream of the Dbx1 gene
- QUANTIFICATION AND STATISTICAL ANALYSIS
- DATA AND CODE AVAILABILITY

SUPPLEMENTAL INFORMATION

Supplemental Information can be found online at <https://doi.org/10.1016/j.celrep.2019.09.007>.

ACKNOWLEDGMENTS

We acknowledge the ImagoSeine facility, a member of the France Biolmaging infrastructure supported by the Agence Nationale de la Recherche (ANR-10-INSB-04, “Investments for the future”), for help with confocal microscopy; An-malliance for technical assistance and animal care; N. Klaus, S. Goebels, S.M. Barnat, and S. Humbert for providing the *Nex-cre* mouse line; S. Karaz, M. Courgeon, and F. Causeret for the pCAGGS-*Dbx1-ires-EGFP* plasmid and sequence; M. Moreau and F. Causeret for interrogating public databases; and J. Fei for providing pCAGGS-*mCherry* and pCAGGS-*loxP-stop-loxP* plasmids. We thank F. Matsuzaki, T. Suetsugu, and A. Shitamukai for training in *ex utero* electroporation; E. Taverna, J. Pulvers, M. Barber, T. Nomura, and J. Sap for critical reading of the manuscript; members of Pierani’s laboratory for discussion; and L. Vigier for mouse maintenance. Y.A. was supported by the ARC (Association pour la Recherche sur le Cancer), FRM (Fondation pour la Recherche Médicale), and JSPS (Japan Society for the Promotion of Science); A.W.C. by the FRM. A.P. is a CNRS (Centre National de la Recherche Scientifique) Investigator and the Team member of the École des Neurosciences de Paris Ile-de-France (ENP). This work was supported by grants from the Agence Nationale de la Recherche (ANR-2011-BSV4-023-01 and ANR-15-CE16-0003-01), FRM (Equipe FRM DEQ20130326521), Fondation ARC pour la Recherche sur le Cancer (ARC, Project ARC SFI20111203674), Ville de Paris (2006 ASES 102), and Fédération pour la Recherche sur le Cerveau (FRC) to A.P.; and state funding from the Agence Nationale de la Recherche under “Investissements d’avenir” program (ANR-10-IAHU-01) to the Imagine Institute and Brain Mapping by Integrated Neurotechnologies for Disease Studies

(Brain/MINDS) from the Ministry of Education, Culture, Sports, Science, and Technology of Japan (MEXT) to H.O.

AUTHOR CONTRIBUTIONS

Y.A. and A.P. conceived the study, analyzed the data, and co-wrote the manuscript. Y.A. performed most of the experiments. A.W.C. performed electroporations and immunostaining in mouse and human, analyzed the data, and performed most of the revisions. E.C. participated in the analysis of transgenic lines and in the revisions. S.C. and Y.S. performed some human immunostaining. H.N. generated marmoset 10 kb transgenic mice. H.K. produced 5 kb and 10 kb marmoset DNA constructs. B.F.-H. performed mouse Dbx1 *in situ* hybridization and Nurr1/Ctip2 immunostaining. A.D. provided mouse colony maintenance. N.O. provided support for the generation of marmoset 10 kb transgenic mice. H.O. and T.S. provided marmoset material, T.S. also expertise in *in utero* electroporation at E11.5. P.G. and J.N. provided an access to donated human fetal tissue. C.D. provided macaque tissue. G.D. performed bioinformatics analyses. A.P. supervised the project. All authors discussed and edited the manuscript.

DECLARATION OF INTERESTS

H.O. is a paid member of the scientific advisory board of SanBio. The remaining authors declare no competing interests.

Received: April 24, 2019

Revised: July 12, 2019

Accepted: September 4, 2019

Published: October 15, 2019

REFERENCES

- Alfano, C., Magrinelli, E., Harb, K., Hevner, R.F., and Studer, M. (2014). Postmitotic control of sensory area specification during neocortical development. *Nat. Commun.* 5, 5632.
- Arai, Y., and Pierani, A. (2014). Development and evolution of cortical fields. *Neurosci. Res.* 86, 66–76.
- Arai, Y., Pulvers, J.N., Haffner, C., Schilling, B., Nüsslein, I., Calegari, F., and Huttner, W.B. (2011). Neural stem and progenitor cells shorten S-phase on commitment to neuron production. *Nat. Commun.* 2, 154.
- Arlotta, P., and Hobert, O. (2015). Homeotic transformations of neuronal cell identities. *Trends Neurosci.* 38, 751–762.
- Bar, I., Lambert de Rouvroit, C., and Goffinet, A.M. (2000). The evolution of cortical development. An hypothesis based on the role of the Reelin signaling pathway. *Trends Neurosci.* 23, 633–638.
- Barber, M., and Pierani, A. (2016). Tangential migration of glutamatergic neurons and cortical patterning during development: lessons from Cajal-Retzius cells. *Dev. Neurobiol.* 76, 847–881.
- Barber, M., Arai, Y., Morishita, Y., Vigier, L., Causeret, F., Borello, U., Ledonne, F., Coppola, E., Contremoulins, V., Pfrieger, F.W., et al. (2015). Migration speed of Cajal-Retzius cells modulated by vesicular trafficking controls the size of higher-order cortical areas. *Curr. Biol.* 25, 2466–2478.
- Bayer, S.A., and Altman, J. (2002). *The Human Brain During the Late First Trimester* (CRC Press).
- Bedogni, F., Hodge, R.D., Elsen, G.E., Nelson, B.R., Daza, R.A.M., Beyer, R.P., Bammler, T.K., Rubenstein, J.L., and Hevner, R.F. (2010). *Tbr1* regulates regional and laminar identity of postmitotic neurons in developing neocortex. *Proc. Natl. Acad. Sci. USA* 107, 13129–13134.
- Betizeau, M., Cortay, V., Patti, D., Pfister, S., Gautier, E., Bellemin-Ménard, A., Afanassieff, M., Huissoud, C., Douglas, R.J., Kennedy, H., and Dehay, C. (2013). Precursor diversity and complexity of lineage relationships in the outer subventricular zone of the primate. *Neuron* 80, 442–457.
- Bielle, F., Griveau, A., Narboux-Nême, N., Vigneau, S., Sigrist, M., Arber, S., Wassef, M., and Pierani, A. (2005). Multiple origins of Cajal-Retzius cells at the borders of the developing pallium. *Nat. Neurosci.* 8, 1002–1012.

- Borello, U., and Pierani, A. (2010). Patterning the cerebral cortex: traveling with morphogens. *Curr. Opin. Genet. Dev.* *20*, 408–415.
- Bouvier, J., Thoby-Brisson, M., Renier, N., Dubreuil, V., Ericson, J., Champagnat, J., Pierani, A., Chédotal, A., and Fortin, G. (2010). Hindbrain interneurons and axon guidance signaling critical for breathing. *Nat. Neurosci.* *13*, 1066–1074.
- Boyd, J.L., Skove, S.L., Rouanet, J.P., Pilaz, L.-J., Bepler, T., Gordán, R., Wray, G.A., and Silver, D.L. (2015). Human-chimpanzee differences in a FZD8 enhancer alter cell-cycle dynamics in the developing neocortex. *Curr. Biol.* *25*, 772–779.
- BrainSpan. (2011). Atlas of the Developing Human Brain, Available at. <https://developinghumanbrain.org>.
- Briscoe, J., and Novitsch, B.G. (2008). Regulatory pathways linking progenitor patterning, cell fates and neurogenesis in the ventral neural tube. *Philos. Trans. R. Soc. Lond. B Biol. Sci.* *363*, 57–70.
- Briscoe, J., Pierani, A., Jessell, T.M., and Ericson, J. (2000). A homeodomain protein code specifies progenitor cell identity and neuronal fate in the ventral neural tube. *Cell* *101*, 435–445.
- Carney, R.S.E., Cocas, L.A., Hirata, T., Mansfield, K., and Corbin, J.G. (2009). Differential regulation of telencephalic pallial-subpallial boundary patterning by Pax6 and Gsh2. *Cereb. Cortex* *19*, 745–759.
- Chen, B., Wang, S.S., Hattox, A.M., Rayburn, H., Nelson, S.B., and McConnell, S.K. (2008). The Fezf2-Ctip2 genetic pathway regulates the fate choice of subcortical projection neurons in the developing cerebral cortex. *Proc. Natl. Acad. Sci. USA* *105*, 11382–11387.
- Chou, S.-J., Perez-Garcia, C.G., Kroll, T.T., and O’Leary, D.D.M. (2009). Lhx2 specifies regional fate in Emx1 lineage of telencephalic progenitors generating cerebral cortex. *Nat. Neurosci.* *12*, 1381–1389.
- Cocas, L.A., Georgala, P.A., Mangin, J.-M., Clegg, J.M., Kessar, N., Haydar, T.F., Gallo, V., Price, D.J., and Corbin, J.G. (2011). Pax6 is required at the telencephalic pallial-subpallial boundary for the generation of neuronal diversity in the postnatal limbic system. *J. Neurosci.* *31*, 5313–5324.
- Corish, P., and Tyler-Smith, C. (1999). Attenuation of green fluorescent protein half-life in mammalian cells. *Protein Eng.* *12*, 1035–1040.
- D’Arcangelo, G., Miao, G.G., Chen, S.C., Soares, H.D., Morgan, J.I., and Curran, T. (1995). A protein related to extracellular matrix proteins deleted in the mouse mutant reeler. *Nature* *374*, 719–723.
- De Carlos, J.A., and O’Leary, D.D. (1992). Growth and targeting of subplate axons and establishment of major cortical pathways. *J. Neurosci.* *12*, 1194–1211.
- De la Rossa, A., Bellone, C., Golding, B., Vitali, I., Moss, J., Toni, N., Lüscher, C., and Jabaudon, D. (2013). In vivo reprogramming of circuit connectivity in postmitotic neocortical neurons. *Nat. Neurosci.* *16*, 193–200.
- Elsen, G.E., Hodge, R.D., Bedogni, F., Daza, R.A.M., Nelson, B.R., Shiba, N., Reiner, S.L., and Hevner, R.F. (2013). The protomap is propagated to cortical plate neurons through an Eomes-dependent intermediate map. *Proc. Natl. Acad. Sci. USA* *110*, 4081–4086.
- Englund, C., Fink, A., Lau, C., Pham, D., Daza, R.A.M., Bulfone, A., Kowalczyk, T., and Hevner, R.F. (2005). Pax6, Tbr2, and Tbr1 are expressed sequentially by radial glia, intermediate progenitor cells, and postmitotic neurons in developing neocortex. *J. Neurosci.* *25*, 247–251.
- Fame, R.M., MacDonald, J.L., Dunwoodie, S.L., Takahashi, E., and Macklis, J.D. (2016). Cited2 regulates neocortical layer II/III generation and somatosensory callosal projection neuron development and connectivity. *J. Neurosci.* *36*, 6403–6419.
- Fietz, S.A., Kelava, I., Vogt, J., Wilsch-Bräuninger, M., Stenzel, D., Fish, J.L., Corbeil, D., Riehn, A., Distler, W., Nitsch, R., and Huttner, W.B. (2010). OSVZ progenitors of human and ferret neocortex are epithelial-like and expand by integrin signaling. *Nat. Neurosci.* *13*, 690–699.
- Fonseca, M., del Río, J.A., Martínez, A., Gómez, S., and Soriano, E. (1995). Development of calretinin immunoreactivity in the neocortex of the rat. *J. Comp. Neurol.* *361*, 177–192.
- Friedrichs, M., Larralde, O., Skutella, T., and Theil, T. (2008). Lamination of the cerebral cortex is disturbed in Gli3 mutant mice. *Dev. Biol.* *318*, 203–214.
- García-Moreno, F., López-Mascaraque, L., and De Carlos, J.A. (2007). Origins and migratory routes of murine Cajal-Retzius cells. *J. Comp. Neurol.* *500*, 419–432.
- Gelman, D.M., and Marín, O. (2010). Generation of interneuron diversity in the mouse cerebral cortex. *Eur. J. Neurosci.* *31*, 2136–2141.
- Ghosh, A., Antonini, A., McConnell, S.K., and Shatz, C.J. (1990). Requirement for subplate neurons in the formation of thalamocortical connections. *Nature* *347*, 179–181.
- Goebbels, S., Bormuth, I., Bode, U., Hermanson, O., Schwab, M.H., and Nave, K.-A. (2006). Genetic targeting of principal neurons in neocortex and hippocampus of NEX-Cre mice. *Genesis* *44*, 611–621.
- Golonzka, O., Nord, A., Tang, P.L.F., Lindtner, S., Ypsilanti, A.R., Ferretti, E., Visel, A., Selleri, L., and Rubenstein, J.L.R. (2015). Pbx regulates patterning of the cerebral cortex in progenitors and postmitotic neurons. *Neuron* *88*, 1192–1207.
- Greig, L.C., Woodworth, M.B., Galazo, M.J., Padmanabhan, H., and Macklis, J.D. (2013). Molecular logic of neocortical projection neuron specification, development and diversity. *Nat. Rev. Neurosci.* *14*, 755–769.
- Griveau, A., Borello, U., Causeret, F., Tissir, F., Boggetto, N., Karaz, S., and Pierani, A. (2010). A novel role for Dbx1-derived Cajal-Retzius cells in early regionalization of the cerebral cortical neuroepithelium. *PLoS Biol.* *8*, e1000440.
- Hansen, D.V., Lui, J.H., Parker, P.R.L., and Kriegstein, A.R. (2010). Neurogenic radial glia in the outer subventricular zone of human neocortex. *Nature* *464*, 554–561.
- Hevner, R.F., Shi, L., Justice, N., Hsueh, Y., Sheng, M., Smiga, S., Bulfone, A., Goffinet, A.M., Campagnoni, A.T., and Rubenstein, J.L. (2001). Tbr1 regulates differentiation of the preplate and layer 6. *Neuron* *29*, 353–366.
- Hill, R.S., and Walsh, C.A. (2005). Molecular insights into human brain evolution. *Nature* *437*, 64–67.
- Hirata, T., Li, P., Lanuza, G.M., Cocas, L.A., Huntsman, M.M., and Corbin, J.G. (2009). Identification of distinct telencephalic progenitor pools for neuronal diversity in the amygdala. *Nat. Neurosci.* *12*, 141–149.
- Hoerder-Suabedissen, A., and Molnár, Z. (2013). Molecular diversity of early-born subplate neurons. *Cereb. Cortex* *23*, 1473–1483.
- Hoerder-Suabedissen, A., and Molnár, Z. (2015). Development, evolution and pathology of neocortical subplate neurons. *Nat. Rev. Neurosci.* *16*, 133–146.
- Kanold, P.O., and Luhmann, H.J. (2010). The subplate and early cortical circuits. *Annu. Rev. Neurosci.* *33*, 23–48.
- Karaz, S., Courgeon, M., Lepetit, H., Bruno, E., Pannone, R., Tarallo, A., Thouzé, F., Kerner, P., Vervoort, M., Causeret, F., et al. (2016). Neuronal fate specification by the Dbx1 transcription factor is linked to the evolutionary acquisition of a novel functional domain. *Evodevo* *7*, 18.
- Karten, H.J. (1997). Evolutionary developmental biology meets the brain: the origins of mammalian cortex. *Proc. Natl. Acad. Sci. USA* *94*, 2800–2804.
- Kazdoba, T.M., Sunnen, C.N., Crowell, B., Lee, G.H., Anderson, A.E., and D’Arcangelo, G. (2012). Development and characterization of NEX- Pten, a novel forebrain excitatory neuron-specific knockout mouse. *Dev. Neurosci.* *34*, 198–209.
- Khaitovich, P., Tang, K., Franz, H., Kelso, J., Hellmann, I., Enard, W., Lachmann, M., and Pääbo, S. (2006). Positive selection on gene expression in the human brain. *Curr. Biol.* *16*, R356–R358.
- King, M.C., and Wilson, A.C. (1975). Evolution at two levels in humans and chimpanzees. *Science* *188*, 107–116.
- Kwan, K.Y., Sestan, N., and Anton, E.S. (2012). Transcriptional co-regulation of neuronal migration and laminar identity in the neocortex. *Development* *139*, 1535–1546.
- Lu, S., Shashikant, C.S., and Ruddle, F.H. (1996). Separate cis-acting elements determine the expression of mouse Dbx gene in multiple spatial domains of the central nervous system. *Mech. Dev.* *58*, 193–202.

- Lukaszewicz, A., Savatier, P., Cortay, V., Giroud, P., Huissoud, C., Berland, M., Kennedy, H., and Dehay, C. (2005). G1 phase regulation, area-specific cell cycle control, and cytoarchitectonics in the primate cortex. *Neuron* 47, 353–364.
- Magnani, D., Hasenpusch-Theil, K., and Theil, T. (2013). Gli3 controls subplate formation and growth of cortical axons. *Cereb. Cortex* 23, 2542–2551.
- Mangale, V.S., Hirokawa, K.E., Satyaki, P.R.V., Gokulchandran, N., Chikbire, S., Subramanian, L., Shetty, A.S., Martynoga, B., Paul, J., Mai, M.V., et al. (2008). Lhx2 selector activity specifies cortical identity and suppresses hippocampal organizer fate. *Science* 319, 304–309.
- Marinescu, V.D., Kohane, I.S., and Riva, A. (2005). The MAPPER database: a multi-genome catalog of putative transcription factor binding sites. *Nucleic Acids Res.* 33, D91–D97.
- McConnell, S.K., Ghosh, A., and Shatz, C.J. (1989). Subplate neurons pioneer the first axon pathway from the cerebral cortex. *Science* 245, 978–982.
- McKenna, W.L., Betancourt, J., Larkin, K.A., Abrams, B., Guo, C., Rubenstein, J.L.R., and Chen, B. (2011). Tbr1 and Fezf2 regulate alternate corticofugal neuronal identities during neocortical development. *J. Neurosci.* 31, 549–564.
- Meyer, G. (2010). Building a human cortex: the evolutionary differentiation of Cajal-Retzius cells and the cortical hem. *J. Anat.* 217, 334–343.
- Meyer, G., Goffinet, A.M., and Fairén, A. (1999). What is a Cajal-Retzius cell? A reassessment of a classical cell type based on recent observations in the developing neocortex. *Cereb. Cortex* 9, 765–775.
- Meyer, G., Schaaps, J.P., Moreau, L., and Goffinet, A.M. (2000). Embryonic and early fetal development of the human neocortex. *J. Neurosci.* 20, 1858–1868.
- Molnár, Z., and Butler, A.B. (2002). The corticostriatal junction: a crucial region for forebrain development and evolution. *BioEssays* 24, 530–541.
- Molyneaux, B.J., Arlotta, P., Menezes, J.R.L., and Macklis, J.D. (2007). Neuronal subtype specification in the cerebral cortex. *Nat. Rev. Neurosci.* 8, 427–437.
- Nakamura, A., Swahiri, V., Plestant, C., Smith, I., McCoy, E., Smith, S., Moy, S.S., Anton, E.S., and Deshmukh, M. (2016). Bcl-xL is essential for the survival and function of differentiated neurons in the cortex that control complex behaviors. *J. Neurosci.* 36, 5448–5461.
- Nomura, T., Takahashi, M., Hara, Y., and Osumi, N. (2008). Patterns of neurogenesis and amplitude of Reelin expression are essential for making a mammalian-type cortex. *PLoS ONE* 3, e1454.
- Ogawa, M., Miyata, T., Nakajima, K., Yagyu, K., Seike, M., Ikenaka, K., Yamamoto, H., and Mikoshiba, K. (1995). The reeler gene-associated antigen on Cajal-Retzius neurons is a crucial molecule for laminar organization of cortical neurons. *Neuron* 14, 899–912.
- Ozair, M.Z., Kirst, C., van den Berg, B.L., Ruvo, A., Rito, T., and Brivanlou, A.H. (2018). hPSC modeling reveals that fate selection of cortical deep projection neurons occurs in the subplate. *Cell Stem Cell* 23, 60–73.e66.
- Pedraza, M., Hoerder-Suabedissen, A., Albert-Maestro, M.A., Molnár, Z., and De Carlos, J.A. (2014). Extracortical origin of some murine subplate cell populations. *Proc. Natl. Acad. Sci. USA* 111, 8613–8618.
- Pierani, A., Brenner-Morton, S., Chiang, C., and Jessell, T.M. (1999). A sonic hedgehog-independent, retinoid-activated pathway of neurogenesis in the ventral spinal cord. *Cell* 97, 903–915.
- Pierani, A., Moran-Rivard, L., Sunshine, M.J., Littman, D.R., Goulding, M., and Jessell, T.M. (2001). Control of interneuron fate in the developing spinal cord by the progenitor homeodomain protein Dbx1. *Neuron* 29, 367–384.
- Price, D.J., Aslam, S., Tasker, L., and Gillies, K. (1997). Fates of the earliest generated cells in the developing murine neocortex. *J. Comp. Neurol.* 377, 414–422.
- Puelles, L. (2011). Pallio-pallial tangential migrations and growth signaling: new scenario for cortical evolution? *Brain Behav. Evol.* 78, 108–127.
- Puelles, L., and Rubenstein, J.L. (1993). Expression patterns of homeobox and other putative regulatory genes in the embryonic mouse forebrain suggest a neuromeric organization. *Trends Neurosci.* 16, 472–479.
- Rakic, P. (2009). Evolution of the neocortex: a perspective from developmental biology. *Nat. Rev. Neurosci.* 10, 724–735.
- Rueda-Alaña, E., Martínez-Garay, I., Encinas, J.M., Molnár, Z., and García-Moreno, F. (2018). Dbx1-derived pyramidal neurons are generated locally in the developing murine neocortex. *Front. Neurosci.* 12, 792.
- Saulnier, A., Keruzore, M., De Clercq, S., Bar, I., Moers, V., Magnani, D., Walcher, T., Filippis, C., Kricha, S., Parlier, D., et al. (2013). The doublesex homolog Dmrt5 is required for the development of the caudomedial cerebral cortex in mammals. *Cereb. Cortex* 23, 2552–2567.
- Schneider, C.A., Rasband, W.S., and Eliceiri, K.W. (2012). NIH Image to ImageJ: 25 years of image analysis. *Nat. Methods* 9, 671–675.
- Schuermans, C., and Guillemot, F. (2002). Molecular mechanisms underlying cell fate specification in the developing telencephalon. *Curr. Opin. Neurobiol.* 12, 26–34.
- Shirasaki, R., and Pfaff, S.L. (2002). Transcriptional codes and the control of neuronal identity. *Annu. Rev. Neurosci.* 25, 251–281.
- Siepel, A., and Arbiza, L. (2014). Cis-regulatory elements and human evolution. *Curr. Opin. Genet. Dev.* 29, 81–89.
- Smart, I.H.M., Dehay, C., Giroud, P., Berland, M., and Kennedy, H. (2002). Unique morphological features of the proliferative zones and postmitotic compartments of the neural epithelium giving rise to striate and extrastriate cortex in the monkey. *Cereb. Cortex* 12, 37–53.
- Sokolowski, K., Esumi, S., Hirata, T., Kamal, Y., Tran, T., Lam, A., Oboti, L., Brighthaupt, S.C., Zaghulua, M., Martinez, J., et al. (2015). Specification of select hypothalamic circuits and innate behaviors by the embryonic patterning gene dbx1. *Neuron* 86, 403–416.
- Srinivasan, K., Leone, D.P., Bateson, R.K., Dobrova, G., Kohwi, Y., Kohwi-Shigematsu, T., Grosschedl, R., and McConnell, S.K. (2012). A network of genetic repression and derepression specifies projection fates in the developing neocortex. *Proc. Natl. Acad. Sci. USA* 109, 19071–19078.
- Stenman, J., Yu, R.T., Evans, R.M., and Campbell, K. (2003). Tlx and Pax6 cooperate genetically to establish the pallio-subpallial boundary in the embryonic mouse telencephalon. *Development* 130, 1113–1122.
- Sumiyama, K., Kawakami, K., and Yagita, K. (2010). A simple and highly efficient transgenesis method in mice with the Tol2 transposon system and cytoplasmic microinjection. *Genomics* 95, 306–311.
- Supèr, H., Soriano, E., and Uylings, H.B. (1998). The functions of the preplate in development and evolution of the neocortex and hippocampus. *Brain Res. Brain Res. Rev.* 27, 40–64.
- Takiguchi-Hayashi, K., Sekiguchi, M., Ashigaki, S., Takamatsu, M., Hasegawa, H., Suzuki-Migishima, R., Yokoyama, M., Nakanishi, S., and Tanabe, Y. (2004). Generation of reelin-positive marginal zone cells from the caudomedial wall of telencephalic vesicles. *J. Neurosci.* 24, 2286–2295.
- Tashiro, K., Teissier, A., Kobayashi, N., Nakanishi, A., Sasaki, T., Yan, K., Tarabykin, V., Vigier, L., Sumiyama, K., Hirakawa, M., et al. (2011). A mammalian conserved element derived from SINE displays enhancer properties recapitulating Satb2 expression in early-born callosal projection neurons. *PLoS ONE* 6, e28497.
- Teissier, A., Griveau, A., Vigier, L., Piolot, T., Borello, U., and Pierani, A. (2010). A novel transient glutamatergic population migrating from the pallial-subpallial boundary contributes to neocortical development. *J. Neurosci.* 30, 10563–10574.
- Tissir, F., Ravn, A., Achouri, Y., Riethmacher, D., Meyer, G., and Goffinet, A.M. (2009). DeltaNp73 regulates neuronal survival in vivo. *Proc. Natl. Acad. Sci. USA* 106, 16871–16876.
- Viswanathan, S., Bandyopadhyay, S., Kao, J.P.Y., and Kanold, P.O. (2012). Changing microcircuits in the subplate of the developing cortex. *J. Neurosci.* 32, 1589–1601.

- Waclaw, R.R., Ehrman, L.A., Pierani, A., and Campbell, K. (2010). Developmental origin of the neuronal subtypes that comprise the amygdalar fear circuit in the mouse. *J. Neurosci.* *30*, 6944–6953.
- Wu, S.-X., Goebbels, S., Nakamura, K., Nakamura, K., Kometani, K., Minato, N., Kaneko, T., Nave, K.A., and Tamamaki, N. (2005). Pyramidal neurons of upper cortical layers generated by NEX-positive progenitor cells in the subventricular zone. *Proc. Natl. Acad. Sci. USA* *102*, 17172–17177.
- Yoshida, M., Assimakopoulos, S., Jones, K.R., and Grove, E.A. (2006). Massive loss of Cajal-Retzius cells does not disrupt neocortical layer order. *Development* *133*, 537–545.
- Yun, K., Potter, S., and Rubenstein, J.L. (2001). Gsh2 and Pax6 play complementary roles in dorsoventral patterning of the mammalian telencephalon. *Development* *128*, 193–205.
- Zecevic, N., and Rakic, P. (2001). Development of layer I neurons in the primate cerebral cortex. *J. Neurosci.* *21*, 5607–5619.
- Zembrzycki, A., Perez-Garcia, C.G., Wang, C.-F., Chou, S.-J., and O’Leary, D.D.M. (2015). Postmitotic regulation of sensory area patterning in the mammalian neocortex by Lhx2. *Proc. Natl. Acad. Sci. USA* *112*, 6736–6741.

STAR★METHODS

KEY RESOURCES TABLE

REAGENT or RESOURCE	SOURCE	IDENTIFIER
Antibodies		
DAPI (4', 6-diamidino-2-phenylindole)	Invitrogen Molecular Probes	
Monoclonal Rabbit Anti Dbx1	Pierani et al., 2001	N/A
Polyclonal Rabbit Anti Pax 6	Proteintech	#12323-1-AP
Polyclonal Rabbit Anti GABA	Sigma	#A2052
Monoclonal Mouse Anti GABA	Sigma	#A2082
Polyclonal Rabbit Tbr1	Abcam	#ab31940
Polyclonal Rabbit Tbr2	AbCys S.A	#VPA9618
Polyclonal Rabbit Cre recombinase	Covance	#PRB-106C
Polyclonal Rabbit Calretinin for mouse	Sawant	#7699/3H
Polyclonal Rabbit Calretinin for human	Sawant	#7699/4
Monoclonal Mouse Calretinin for macaque	Sawant	#6B3
Monoclonal Mouse Reln clone G10	Millipore	#MAB5364
Monoclonal Mouse Reln clone 142	Millipore	#MAB5366
Monoclonal Mouse Tuj1	Bio Legend	#MMS-435P
Polyclonal Goat Nurr1	R&D systems	#AF2156
Monoclonal Rat Ctip2	Abcam	#ab18465
Polyclonal Chicken Tbr2	Millipore	#AB15894
Polyclonal Chicken GFP	Aves labs	#GFP-1020
Monoclonal Rat Neural cell adhesion molecule L1	Millipore	#MAB5272
Biological Samples		
Macaca mulatta embryos	Lukaszewicz et al., 2005	N/A
Human embryos GW 6.5	Maternity and Fetopathology departments, Robert Debre Hospital, Paris	N/A
Critical Commercial Assays		
mMESSAGE mMACHINE kit	Life Technologies	#AM1344
DIG-RNA labeling kit	Roche	# 11277073910
Experimental Models: Organisms/Strains		
C57BL/6J pregnant females	Janvier Labs	C57BL/6J
<i>Nex^{Cre}</i> embryos	Goebbels et al., 2006	N/A
Oligonucleotides		
Antisense RNA probes for Dbx1	Pierani et al., 2001	N/A
Marmosets DNAs (template)	Drs. Shiozawa and Imamura from H. Okano laboratory	N/A
Primer: marmoset 10kb-EGFP 5'-CTCCTTACAATT TTATTTACAGTCAAAAAG-3' (forward)	This paper	N/A
Primer: marmoset 10kb-EGFP 5'-GTGACCAGCCT GTATTTAGATACAT-3' (reverse)	This paper	N/A
Primer: marmoset 10kb-EGFP 5'-TTCTAGTTGCCA GCCATCTGTTGTT-3' (forward)	This paper	N/A
Primer: marmoset 10kb-EGFP 5'-TCCATTAATAATT GTACTTGAGTATTAGATC-3' (reverse)	This paper	N/A
Recombinant DNA		
pCAGGS-ires-EGFP	Addgene	#32482
pCAGGS-HA-mouseDbx-ires-EGFP	This paper	N/A

(Continued on next page)

Continued

REAGENT or RESOURCE	SOURCE	IDENTIFIER
pCAGGS-loxP-stop-loxP-EGFP	gift from Dr. Fei	N/A
pCAGGS-loxP-stop-loxP-HA-mouseDbx1-ires-EGFP	This paper	N/A
pCAGGS-ires-NLS-EGFP vector	Karaz et al., 2016	N/A
pCAGGS-HA-mouseDbx1-ires-NLS-EGFP	This paper	N/A
HA-mouseDbx1-ires-NLS-EGFP	This paper	N/A
pCAGGS-mcherry	Addgene	#41583
mouse 5kb-EGFP	This paper	N/A
marmoset 5kb-EGFP	This paper	N/A
marmoset 10kb-EGFP	This paper	N/A
pCS-TP plasmid	Sumiyama et al., 2010	N/A
pBluescript II KS+	Stratagene	#212207
pEF-myc-nuc	Invitrogen	#V89120
Software and Algorithms		
Adobe Photoshop	Adobe	https://www.adobe.com/products/photoshop.html
Excel	Microsoft	Microsoft
Graph Prism	GraphPad Software	https://www.graphpad.com/scientific-software/prism/
Adobe Illustrator	Adobe	https://www.adobe.com/products/illustrator.html
ImageJ	Schneider et al., 2012	https://imagej.nih.gov/ij/
VISualization Tools for Alignments	VISTA	http://genome.lbl.gov/cgi-bin/VistaInput
Multi-genome Analysis of Positions and Patterns of Elements of Regulation	Marinescu et al., 2005	http://genome.ufl.edu/mapper
UCSC	UCSC	https://genome.ucsc.edu
Other		
Mowiol 4-88	Sigma	#81381-50G
Fluoromount-G mounting medium	SouthernBiotech	#0100-01
DAPI (4', 6-diamidino-2-phenylindole)	Invitrogen Molecular Probes (Thermo Fisher)	# D1306
EdU (5-ethynyl-2'-deoxyuridine)	Invitrogen	#E10187

LEAD CONTACT AND MATERIALS AVAILABILITY

Further information and requests for resources and reagents should be directed to and will be fulfilled by the Lead Contact, Alessandra Pierani (alessandra.pierani@inserm.fr). All unique/stable reagents generated in this study are available from the Lead Contact with a completed Materials Transfer Agreement.

EXPERIMENTAL MODEL AND SUBJECT DETAILS

Animals

Dbx1^{iresCre} ([Bielle et al., 2005](#)) were crossed with *ROSA26^{loxP-STOP-loxP-YFP}* (Jackson Laboratory) reporter line to permanently label *Dbx1* lineages. C57BL/6J pregnant females were purchased from JANVIER LABS and *Nex^{Cre}* embryos ([Goebbels et al., 2006](#)) obtained by overnight mating of heterozygous *Nex^{Cre}* males with C57BL/6J females. Noon of the day on which the vaginal plug was observed was defined as embryonic day (E) 0.5. All animals were handled in strict accordance with good animal practice as defined by the national animal welfare bodies, and all mouse work was approved by the Veterinary Services of Paris (Authorization number: 75-1454) and approved by the Animal Experimentation Ethical Committee Buffon (CEEA-40) (Reference: CEB-34-2012).

Two fetuses from cynomolgus monkeys (*Macaca fascicularis*) of known gestational dates (E48 and E49) were delivered as previously described ([Lukaszewicz et al., 2005](#)). All experiments were in compliance with national and European laws as well as with institutional guidelines concerning animal experimentation as described previously ([Betizeau et al., 2013](#)). Surgical procedures

were in accordance with European requirements 2010/63/UE. The protocol C2EA42-12-11-0402-003 has been reviewed and approved by the Animal Care and Use Committee CELYNE (C2EA 42).

One human embryo was collected after legal abortion at gestational week (GW) 6.5. Gestational age was estimated on the basis of pregnancy and anatomy records. Post-mortem delay was less than two hours. All procedures were approved by the ethics committee (Agence de Biomédecine, approval PFS12-0011).

METHOD DETAILS

Immunofluorescence

Mice were sacrificed by cervical dislocation and embryos were collected and fixed at 4°C for 24 hours in 4% paraformaldehyde (PFA), cryoprotected in 30% sucrose in PBS and embedded in Tissue-Tek O.C.T compound (Sakura Finetek, Europe). Brain hemisphere of cynomolgus monkeys (*Macaca fascicularis*) were fixed in 4% PFA for 4 hours, cryoprotected using a progressive sucrose gradient up to 20%, and embedded in Tissue-Tek O.C.T compound. Cryostat coronal sections of mouse embryos (12 μm) and sagittal sections of macaque (30 μm) were rehydrated with PBS, and incubated for 1 hour at 65°C in antigen retrieval solution (10% v/v glycerol in 10 mM sodium citrate, pH 6.0) and cooled down for 20 min at room temperature (r.t.). Sections were permeabilized with 0.1% Triton X-100 in 1% horse serum /1x PBS (HB buffer) for 10 min 3 times and blocked with HB buffer for 30 min at r.t. Sections were subsequently incubated overnight at 4°C with the first primary antibody, followed by incubation for 45 minutes at r.t. with fluorescently labeled secondary antibody and DAPI (4', 6-diamidino-2-phenylindole (Invitrogen Molecular Probes) in HB buffer. Sections were mounted with Mowiol 4-88 reagent (Calbiochem).

Human tissues were fixed for 8 hours in 4% PFA, cryoprotected in 20% sucrose and stored at –80°C until use. Samples were cut into 12 μm sagittal sections, mounted on super-frost slides and stored at –80°C. For Dbx1 staining, an antigen retrieval step was carried out before the permeabilization of sections using HB buffer. With the exception of immunostaining with an anti-Dbx1 antibody, sections were permeabilized with 0.1% Triton X-100 dissolved in 0.12 M phosphate buffer saline (TBS-T) for 15 minutes at r.t., and incubated in blocking buffer solution (10% goat serum in TBS-T) for 1 hour at r.t. to block non-specific binding. Samples were subsequently treated with primary antibodies in blocking buffer for 16 hours at 4°C followed by fluorescently labeled secondary antibodies and DAPI. Coverslips were mounted using Fluoromount-G mounting medium (SouthernBiotech, Birmingham, USA).

The following primary antibodies were used: rabbit antibodies against Dbx1 (Pierani et al., 2001) (1:10000), Pax6 (12323-1-AP, Proteintech; 1:200), GABA (A2052, Sigma; 1:2000 for mouse and A2082, Sigma; 1:500 for human), Tbr1 (ab31940, Abcam; 1:1000), Tbr2 (VPA9618, AbCys S.A.; 1:1000), Cre recombinase (PRB-106C, Covance; 1:2000), Calretinin (7699/3H, Swant; 1:1000 for mouse and 7699/4, Swant; 1:2000 for human); mouse monoclonal antibodies against Reln (clone G10, MAB5364, Millipore; 1:1000 for mouse), Reln (clone 142, a gift from Dr. Goffinet; 1:1000 for human and macaque), Calretinin (6B3, Swant; 1:1000 for macaque), Tuj1 (BAbCo; 1:2000); a goat antibody against Nurr1 (AF2156, R&D systems; 1:200); a rat antibody against Ctip2 (ab18465, Abcam; 1:1000); chick antibodies against Tbr2 (AB15894, Millipore; 1:500), GFP (GFP-1020, Aves labs; 1:2000) and Neural cell adhesion molecule L1 (MAB5272, Millipore; 1:1000). Note that rabbit Dbx1 antibody was raised against the mouse C-terminal 15 aa peptide (DEDEEGEEDDEEITVS), which is conserved between human (80%) and macaque (80%).

All fluorescence images and tilescan images were acquired using a Zeiss Axiovert LSM 710 confocal microscope equipped with Plan-Apochromat 10x NA 0.3 and LDLCI Plan-Apochromat 25x NA 0.8 objectives (Carl Zeiss, Germany), analyzed with ImageJ (<https://imagej.nih.gov/ij/>) and imported into Adobe Photoshop for quantifications.

In situ hybridization

In situ hybridization was performed as previously described (Griveau et al., 2010). Antisense RNA probes for *Dbx1* (Pierani et al., 2001) were labeled using a DIG-RNA labeling kit (Roche).

Exo-in utero electroporation

WT pregnant mice at E11.5 were subjected to abdominal incision under anesthesia with Isoflurane (AXIENCE SAS), and the uterine horns were exposed onto a 1xPBS-moistened cotton gauze. Embryos were visualized using appropriate flexible light sources through the yolk sac and uterus (in some experiments incisions on the uterus were performed to better visualize the embryos). No differences were found by using the two methods and thus most of the experiments were done using exo-utero which is more efficient at these early embryonic stages. Plasmid DNAs mixed with a filtered Fast Green dye were injected into the lateral ventricle through a glass capillary. A pair of electrodes was applied to the embryos through the yolk sac, and a series of square-wave current pulses (25 V, 50 ms) was delivered for six times at 950 ms intervals using a pulse generator (NEPA21, NEPAGENE). Uterine horns were repositioned into the abdominal cavity, and the abdominal wall and skin were sutured. The concentration of plasmid DNAs used were between 1–2.5 μg/ml. *pCAGGS-mcherry* was a gift from Dr. Fei in the CRTD, Dresden, Germany.

EdU pulse labeling and staining

EdU injection was carried out by intraperitoneal injection of 100 μL of 1 mg/ml EdU (Invitrogen) in PBS into pregnant females at E12.5 after electroporation at E11.5 and embryos sacrificed at E14.5. Immunofluorescence and EdU staining was performed as described previously (Arai et al., 2011).

Cloning of marmoset 5 and 10kb genomic DNA sequences

The ~5.3-kb region (“3’ Fragment”) immediately upstream of the marmoset *Dbx1* coding sequence and the ~4.7-kb further upstream region (“5’ Fragment”) were cloned by PCR from genomic DNAs of common marmosets (*Callithrix jacchus*) (gifts from Drs. Shiozawa and Imamura from H. Okano laboratory) as template. The 3’ Fragment was first cloned into pBluescript II KS(+) (Stratagene) backbone vector at the *Bam*H I/*Not* I sites. *Not* I/*Eag* I-cut bovine growth hormone polyadenylation sequence (from the pEF-myc-nuc plasmid (Invitrogen)) was then inserted at the *Not* I site. The construct was re-cut with *Not* I and the enhanced Green Fluorescent Protein (EGFP) coding sequence (from pEGFP-N1 (Clontech)) was inserted. This construct corresponds to the 5kb marmoset promoter construct. The 10kb marmoset promoter construct was generated by inserting *Sall*/*Bam*H I-cut “5’ Fragment” into the corresponding sites in the 5kb marmoset construct.

Generation of 10kb marmoset transgenic mice

Transgenic mice were produced by the *Tol2*-mediated cytoplasmic injection method (Sumiyama et al., 2010). The donor DNA harboring the two *Tol2* transposon recognition sequences flanking the *marmoset 10kb-EGFP* was constructed. The *Tol2* transposase mRNA was synthesized using the mMESSAGING mMACHINE kit (Life Technologies) from the pCS-TP plasmid (Sumiyama et al., 2010). Microinjection solution containing 5 mM Tris-HCl (pH 7.5) and 0.1 mM EDTA, as well as 20 ng/μl donor DNA and 27.5 ng/μl *Tol2* mRNA, was prepared in DEPC-treated water. The solution was filtered with 0.22 μm membrane and used for microinjection according to a standard protocol (Sumiyama et al., 2010; Tashiro et al., 2011). Briefly, cytoplasmic injection was carried out into fertilized eggs of B6C3F1 mice under a microscope, and the microinjected zygotes were transferred to the oviduct of pseudopregnant ICR female mice. Transgene integration and germline transmission were confirmed by PCR-based genotyping to detect the terminal regions of the construct using the 5’-CTCCTTACAATTTTATTACAGTCAAAAAG-3’ (forward) and 5’-GTGACCAGCCTGTATTTAGATACAT-3’ (reverse) primers, and 5’-TTCTAGTTGCCAGCCATCTGTTGTT-3’ (forward) and 5’-TCCATTAATAATTGACTTGAGTATTA GATC-3’ (reverse) primers sets. We obtained 4 founders with germline transmission.

Cloning of *Dbx1* overexpression and Cre-inducible expression vectors

Dbx1 overexpression vectors were based on the pCAGGS vector (a gift from Dr. Briscoe). pCAGGS-HA-mouse*Dbx1*-ires-NLS-EGFP was constructed as follows: a HA-tag was added at the N terminus of the mouse *Dbx1* coding sequence (Pierani et al., 2001) by PCR and inserted in the *Sma*I/*Nhe* I site of the pCAGGS-ires-NLS-EGFP vector (Karaz et al., 2016). The pCAGGS-loxP-stop-loxP-HA-mouse*Dbx1*-ires-NLS-EGFP was constructed as follows: the pCAGGS-HA-mouse*Dbx1*-ires-NLS-EGFP was partially digested by *Xho*I/*Hind*III (1:25 dilution) for 30 min at 37°C to obtain the HA-mouse*Dbx1*-ires-NLS-EGFP fragment. This *Xho*I/*Hind*III fragment was inserted into the 5’ *Xho* I and 3’ *Hind* III sites of the pCAGGS-loxP-stop-loxP vector (a gift from Dr. Fei in the CRTD, Dresden, Germany).

Multiple alignments of genomic sequences upstream of the *Dbx1* gene

The sequence of the developing brain homeobox protein *Dbx1* of mouse (*Mus musculus* NM_001005232) was recovered from the NCBI database (<https://www.ncbi.nlm.nih.gov/>) and used as a query sequence to retrieve orthologous sequences from several vertebrates: human (*Homo sapiens*, NM_001029865.2), marmoset (*Callithrix jacchus*, XM_002807323), rhesus monkey (*Macaca mulatta* XM_002808073) and ferret (*Mustela putorius*, XM_004800385). Using the BLAST tools of the UCSC database (<https://genome.ucsc.edu/>), each *Dbx1* sequence was localized in the corresponding whole genome sequence and the 10kb at the 5’-flanking region of the gene (showing no gaps and/or ambiguous nucleotides) was recovered. All the flanking regions were aligned by VISTA (VISualization Tools for Alignments <http://genome.lbl.gov/cgi-bin/VistaInput>) using default parameters. The VISTA alignment in Figure 2A shows regions with a homology higher than 50%. MAPPER₂ - Multi-genome Analysis of Positions and Patterns of Elements of Regulation (<http://genome.ufl.edu/mapper/>) database (Marinescu et al., 2005) was used to retrieve putative transcription factor (TF) binding sites. 10kb upstream sequences of mouse, marmoset and human *Dbx1* gene were compared, and TF binding sites specifically conserved in both human and marmoset were selected as primary candidates. We then categorized them depending on their genomic location between -5.3 and -10 kb and further selected TFs binding whose binding site was positioned at conserved locations within the -5.3 to -10 kb elements.

QUANTIFICATION AND STATISTICAL ANALYSIS

All the quantifications were made in the DP (anatomically separated from the VP by drawing a straight line at the lateral morphological hinge) or DP and VP. For Figure 2E all mCherry⁺ electroporated cells dorsal to this line were counted and EGFP⁺mCherry⁺ double positive cells were scored as % of the total mCherry⁺ cells. CP, IZ, SVZ and VZ were defined using DAPI⁺ staining and mCherry⁺ fibers as follows: CP, round and packed nuclei located in the uppermost part of the cortex; IZ, horizontally located nuclei and fibers; SVZ, roundish nuclei and multipolar type of fibers, and VZ, radially oriented nuclei and radial fibers in the deeper most part of the cortex. Ctip2⁺EGFP⁺ and Ctip2⁻EGFP⁺ cells in Figure 3E were counted in the entire pallium (DP and VP). For Figures 4, 5, and S4A cells co-expressing analyzed markers together with the EGFP were scored as % of the total EGFP⁺ electroporated cells in the DP.

For all experiments, results were obtained using at least 3 embryos from two or more litters (except for [Figure S4A](#), $n = 1$). For each embryo 1-9 sections were used. Datasets were analyzed using Excel (Microsoft, Redmond, WA) and GraphPad Prism (La Jolla, CA). Statistical tests: for two groups of observations, the unpaired t test, two tails was used for non-parametric analysis. For three groups, the one-way Analysis of Variance (ANOVA) with Tukey's Multiple Comparison test was used for parametric analysis. Results were interpreted as statistically significant when $p < 0.05$.

DATA AND CODE AVAILABILITY

This study did not generate any unique datasets or code.